NASA CONTRACTOR REPORT

NASA CR-984

NASA CR-984

LUNAR ORBITER III

PHOTOGRAPHY

Prepared by
THE BOEING COMPANY
Seattle, Wash.
for Langley Research Center

NATIONAL AERONAUTICS AND SPACE ADMINISTRATION • WASHINGTON, D. C. • FEBRUARY 1968

NASA CR-984

LUNAR ORBITER III

PHOTOGRAPHY

Issued by Originator as Document No. D2-100753-2 (Vol. II)

Prepared under Contract No. NAS 1-3800 by
THE BOEING COMPANY
Seattle, Wash.

for Langley Research Center

NATIONAL AERONAUTICS AND SPACE ADMINISTRATION

For sale by the Clearinghouse for Federal Scientific and Technical Information
Springfield, Virginia 22151 – CFSTI price $3.00

CONTENTS

CONTENTS

FIGURES

FIGURES

FIGURES

TABLES

LUNAR ORBITER III
PHOTOGRAPHY

INTRODUCTION

This volume of the Lunar Orbiter final report contains a description of Mission III planning, its conduct with respect to photography, and an analysis of the photographic results. Data pertinent to analysis and interpretation of the photographs by the user are included. A detailed functional description of the spacecraft photo subsystem and the ground reconstruction is not included in this report, but may be found in Lunar Orbiter Mission I Final Report, NASA Document CR-847. Changes and modifications based on Mission I results are described in Lunar Orbiter Mission II Final Report, NASA Document CR (to be published). Additional changes made for Mission III are discussed in this report.

The telephoto coverage provided resolution equivalent to 1 meter from a nominal altitude of 46 kilometers. In addition to normal near-vertical photography, photographs were obtained with convergent telephoto stereo coverage. Oblique-angle photography was employed to enhance intrepretation of topographic features, to provide photographs of areas beyond the field of view of a vertical camera orientation, and to investigate photometric characteristics of the lunar surface.

Operation of the cameras was satisfactory and high-quality photographs were obtained. Some difficulty was encountered initially during Priority Readout Sequence 25 when a framelet was scanned repeatedly. This problem was intermittent throughout priority and final readout. A second, unrelated difficulty with the readout film advance eventually resulted in termination of final readout before all frames had been read out.

Termination of final readout occurred on March 2, 1967, at 06:36 GMT during readout of Telephoto Frame 79. Of the 74 frames not reached in final readout, a total of 51 were read out in whole or in part by priority readout. By combining priority and final readouts, 82.8% of the planned primary-site, wide-angle coverage and 70.3% of the telephoto coverage was obtained.

1.0 PHOTOGRAPHIC MISSION DESCRIPTION

1.1 PROJECT OBJECTIVES

Lunar Orbiter's primary objective is to provide information necessary to locate sites that meet the requirements for Apollo manned lunar landings. These requirements include the following.

- Certification of multiple sites providing for accessibility during different Apollo launch windows and recycle times (at least 2 days between launch attempts and three launch attempts each month);
- Location of areas—free of protuberances, depressions, or slopes constituting a hazard to landing—that are large enough to accommodate Lunar Module guidance errors and maneuver capabilities;
- The locations must be within the zone of ±5° latitude and ±45° longitude.

Secondary objectives are to provide data regarding the lunar environment, including energetic radiation and meteoroid flux, and selenodesy and the Moon's gravitational field by determination of spacecraft orbit characteristics and perturbations.

1.2 MISSION III PHOTOGRAPHIC OBJECTIVES

The primary objective of Mission III was essentially unchanged from that of the prior missions: i.e., to obtain topographic informa-

tion of various lunar areas to assess their suitability for use as Apollo and Surveyor landing sites. As stated explicitly by NASA in LOTD-113-0, the objectives are:

- Primary— To obtain, from lunar orbit, detailed photographic information of various lunar areas, to assess their suitability as landing sites for Apollo and Surveyor spacecraft, and to improve our knowledge of the Moon.

- Secondary—To provide precision trajectory information for use in improving the definition of the lunar gravitation field. To provide measurements of micrometeroid flux and radiation dose in the lunar environment, primarily for spacecraft performance analysis.
  To provide a spacecraft which can be tracked in lunar orbit by the MSFN stations for the purpose of exercising and evaluating the tracking network and Apollo Orbit Determination program.

The basic difference between Mission III and the previous two missions is that Mission III is primarily a site-confirmation mission rather than a site-search mission.

During Mission II it was demonstrated that photography of areas away from the orbital track by oblique line of sight was feasible, and evaluation of the resulting photographs proved their great value. The experience thus gained in Mission II led to the plan to photograph, where possible as secondary sites, locations that were of special scientific interest not necessarily related to the Apollo landing.

1.3 PHOTOGRAPHIC MISSION SUMMARY

Liftoff of the Lunar Orbiter occurred February 5, 1967, at 05:17:17:01.12 GMT. Following the cislunar portion of flight, the spacecraft was injected into its initial orbit at 21:54:19 GMT on February 8, 1967. The orbit achieved had the following initial parameters.

	Orbit 0*	Orbit 1
Apolune	1802.1 km	1802.0 km
Perilune	210.3 km	210.2 km
Inclination	20.96 deg	21.05 deg
Period	215.0 min	215.0 min

*Note: Orbit 0 is the portion of initial orbital path extending from injection point to apolune where Orbit 1 commences.

Transfer to the second ellipse was accomplished February 12 at 18:14 GMT during Orbit 25. The initial parameters of the second ellipse (photographic) for Orbit 26 were:

Apolune	1847.2 km
Perilune	54.9 km
Inclination	20.86 deg
Period	208.56 min

The leading end of the film in the camera subsystem included a section of pre-exposed and preprocessed film having a test image. This section was included to provide an initial verification of readout operation and quality evaluation.

Readout of the test film occurred during Orbits 39 and 40 and again during Orbit 43. Results of the readout were excellent. The first photographs were taken February 15 during Orbit 44 at 10:00 GMT. A sequence of 16 frames in fast mode was exposed over Site IIIP-1, followed by a sequence of four at Site IIIS-1.

Mission photography was completed and Bimat cut was made at 06:36 GMT on February 23. Table 1-1 summarizes mission photography.

Sites IIIP-3 and IIIP-6, both four-frame sequences, were exposed using the slow mode. Fast-mode sequencing was used at all other primary sites. Of the eight secondary sites for which four-frame sequences were

Table 1-1: ALLOCATION OF PHOTOGRAPHIC FRAMES

Primary Sites

No. of Sequences	Sites	Frames per Sequence	Total Frames
2	P-1, -12a	16	32
13	P-2a, -4, -5a, -5b, -7a, -7b, -8, -9a, -9b, -9c, -10, -11, -12c	8	104
5	P-2b, -3, -6, -12b.2, -12b.1	4	20

Secondary Sites

8	S-1, -7, -10, -15, -17, -18, -19, -23	4	32
23	(See Table 3-4)	1	23
			211

Secondary-Site Photography

Oblique	30 frames
Vertical	23 frames (tilt<10 degrees)
Farside	2 frames

exposed, Sites IIIS-1 and IIIS-18 were sequenced in the fast mode to obtain contiguous telephoto coverage. The remainder were sequenced in the slow mode, providing approximately 50% overlapping wide-angle coverage.

All mission targets were selected and photography planned prior to flight; however, some modifications were made in target location and in the photographic procedures to be used at particular sites. The location for Site IIIP-12, the Surveyor I site, was changed on the basis of revised location prediction from the Surveyor Project. The location of Site IIIP-7 was changed for spacecraft operational reasons. The locations and photographic procedures were modified for Sites IIIP-9, -11, and -12, and for six secondary sites. Details of these changes are included in Section 2.0.

All photography planned for the mission (except for the last secondary site, which was deleted) was accomplished successfully. The last secondary site was deleted to allow final readout to be started sooner than had been planned, because of the problem of film hangup during priority mode readout.

The intermittent problem with readout film movement continued during final readout. On March 2 at 06:36 GMT, as a result of a logic failure caused by an unknown transient, film advance beyond Telephoto Frame 79 could not be made and final readout was terminated. A technical analysis and report on this failure will be found in Volume III of this final report.

1.4 PHOTOGRAPHIC SUBSYSTEM DESCRIPTION

A description of the Lunar Orbiter photographic subsystem and its functions, together with ground support equipment necessary for reconstruction of photographs, has been included in Lunar Orbiter Mission I Final Report, Volume II. Changes made for the second mission, also incorporated in the photo subsystem for Mission III, are described in Lunar Orbiter Mission II Final Report, Volume II. Discussion here will be limited to additional changes made prior to Mission III that are pertinent to the photographic results, to significant factors specific to Mission III, and to procedural changes in preparation of the photographs.

1.4.1 Spacecraft Photographic Subsystem

Changes in the photo subsystem for Mission II to correct the focal-plane shutter operation and other problems encountered in Mission I were also included in the photo subsystem for Mission III. Major improvements for Mission III include a modification of the reseau mark pattern pre-exposed on the spacecraft film, and the installation of a neutral-density filter in the wide-angle camera to equalize exposure with the telephoto lens.

1.4.1.1 Reseau Marks

A pre-exposed pattern of reseau marks was placed on the spacecraft film for Mission II to provide a means for determination and correction of image distortions introduced by the system subsequent to the optical imaging on the spacecraft film. The pattern of the reseau marks was changed for Mission III to provide a closer pattern to improve measurement capability. The pattern used for Mission III is illustrated in Figure 1-1. The placement ensures that two lines of reseau marks will appear along the length of each framelet.

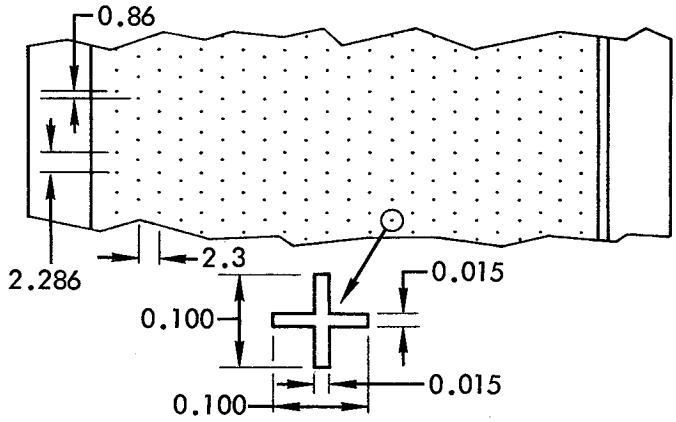

Figure 1-1: Pre-exposed Reseau Mark Placement and Detail of Cross

It will also be noted that the width of the lines forming the cross (0.015 mm on the spacecraft film) is equivalent to approximately 1.5 meters on the ground in telephoto pictures where the distance from the camera is about 50 kilometers. This relationship is suitable only for visual approximation of ground detail size and should not be the basis for quantitative measurement since the apparent dimensions may be affected by system resolution limitation.

1.4.1.2 Neutral-Density Filter

The 80-mm wide-angle camera lens was equipped with a 0.21 neutral-density filter to correct for the light transmission differential between this lens and the telephoto lens. The resultant 80-mm-lens transmissivity was 59% compared with 65% for the 610-mm lens. The residual difference was partially compensated by slightly shorter than nominal shutter speeds of the focal-plane shutter. Image density differential between the two cameras was within 0.1 except at exposure extremes.

1.4.2 Calibration

Tests and calibrations performed on the photographic subsystem for Mission III were the same as those for the previous missions, and are described in Lunar Orbiter Mission I Final Report, Volume II. The tests and calibrations include lens-film characteristics, exposure calibration and control, image motion compensation, camera alignment, readout quality, and photogrammetric distortion calibration of the 80-mm camera.

The test and calibration data specific to Mission III has been submitted to NASA. These data, along with copies of the photographs, can be obtained by interested scientists from the National Space Science Data Center of the Goddard Space Flight Center.

2.0 PHOTOGRAPHIC SITES

Photographic sites for Mission III are specified in Lunar Orbiter Project Mission III Description, NASA Document NASA LOTD-113-0, dated January 25, 1967, supplemented by Lunar Orbiter Project Office Memorandum 10M-2928-ATY, dated January 26, 1967. These specifications were revised and corrected by Lunar Orbiter Project Office Memorandum 10M-67-292-ATY/NLC, dated February 21, 1967. Changes specified in the third reference above were received after mission photography had started.

Orbit design for Mission III was the same as for Missions I and II except that the orbit inclination was increased from 12 to 21 degrees. Although the increased inclination eliminates the possibility of obtaining vertical telephoto coverage of every part of the Apollo zone, it increases the latitude range of the zone of acceptable illumination and allows photography in both the northern and southern portions of the Apollo zone. Complete coverage can, however, be achieved by slight tilt of the camera axis. Degradation of resolution caused by the tilt is small.

Guidelines were established for selection of Mission III target sites. These guidelines, as given in LOTD-113-0, were:

"Primary Sites:

A. Provide the additional data now needed to select Surveyor sites in support of Apollo and other candidate sites for the first Apollo mission.
B. Provide the data necessary to screen other candidate landing sites for Surveyor.
C. Provide oblique views of promising Apollo landing sites.
D. Provide data:
   - Necessary to screen potential landing sites for subsequent manned lunar missions.
   - To calibrate the relative roughness of highlands.
   - Of scientific interest."

Secondary sites included in "B," above, are in different terrain types from Apollo support sites, which are all in maria. They provide information of value in selection of nonmare Surveyor landing sites. Mission I and particularly Mission II have demonstrated not only the feasibility but also the value of oblique photography in terrain analysis. Therefore, the amount of oblique photography was substantially increased for Mission III. As stated in LOTD-113-0, the photographs selected under "C," above, "are to provide a pictorial view that has geometric and photometric conditions representative of that which will exist during a manned descent to the landing sites. In addition, the oblique views are to locate landmarks proximal to the site that can be used for reference during Apollo missions." Selection of sites primarily of scientific interest was constrained by film-set and by Bimat stick and dryout limitations or requirements.

Selection of the 12 primary sites for Mission III was based on preliminary analysis by NASA of Lunar Orbiters I and II photographs. Five of the Mission I sites that appeared to be relatively smooth were included in Mission III to obtain high-resolution photographs of these areas. Five of the 13 Mission II primary sites appeared to be sufficiently smooth to justify additional photography under more favorable lighting. The other two primary sites for Mission III were possible Surveyor sites in western Mare Tranquillitatis that were selected on the basis of Earth-based photography.

The specifications for Mission III sites are given in Enclosure A of NASA Letter B/L-1101-NLC dated February 1, 1967. Some modifications were made during the course of the mission, as shown in NASA Memorandum 10M-67-292-ATY/NLC dated February 21, 1967.

Most of the changes involved secondary sites. The main effect of the changes involved modifications of the film management and budgeting discussed in Section 5.1. The photographic procedure for Primary Site IIIP-12 was also modified to improve coverage of the Surveyor I landing site area and is described in detail in Section 3.2.12.

3.0 PHOTOGRAPHS

Assessment of Mission III photographs has been based upon examination of second-generation, 35-mm GRE reconstructed record film positives and of paper prints prepared from hand-reassembled GRE film by NASA and the Army Map Service. Assessment of photographic quality based upon exposure, and estimation of resolution was based on the GRE record. Paper prints were used only to relate topographic characteristics, apparent albedo variations, and illumination to photographic quality of complete frames and sequences; to screen photographs for processing or other anomalies; and to correlate site coverage with lunar charts. Evaluation of complete frames or sequences, and correlation of site characteristics to photography by examination of framelets in the rolls of GRE film, are difficult because of the small relative size of a framelet.

3.1 GENERAL CHARACTERISTICS

Mission III employed a greater diversity of techniques for photography of both primary and secondary sites than used for Missions I and II. On the previous missions, primary sites were photographed with the camera axis oriented near vertical for monoscopic photography in high resolution and stereoscopic photography in wide-angle coverage by overlap of successive frames. One of the Mission II secondary sites was photographed using an experimental technique to obtain high-resolution convergent stereo coverage. This required photography of the same area from two successive orbits, with the camera axis tilted so that the areal coverages with the telephoto lens are coincident.

Because of the success of the above experiment, six of the 12 primary sites were selected for convergent telephoto stereo coverage. The remaining sites were planned for near-vertical photography or with cross-track tilt of the camera axis required for coverage from the nearest orbit. Where convergent stereo photography was used for a primary site, one sequence of photographs was taken with the camera axis near vertical to obtain maximum resolution of the area. The camera axis was tilted on the other pass the amount necessary for coincident coverage. This is illustrated in Figure 3-1. While this technique increased the degradation of resolution caused by the greater tilt for one sequence, such resolution penalty was offset by retaining maximum resolution of the area by the near-vertical coverage. This was the general scheme. In practice, the tilt of the two sequences was determined for the location of the desired site center with respect to the two orbital tracks.

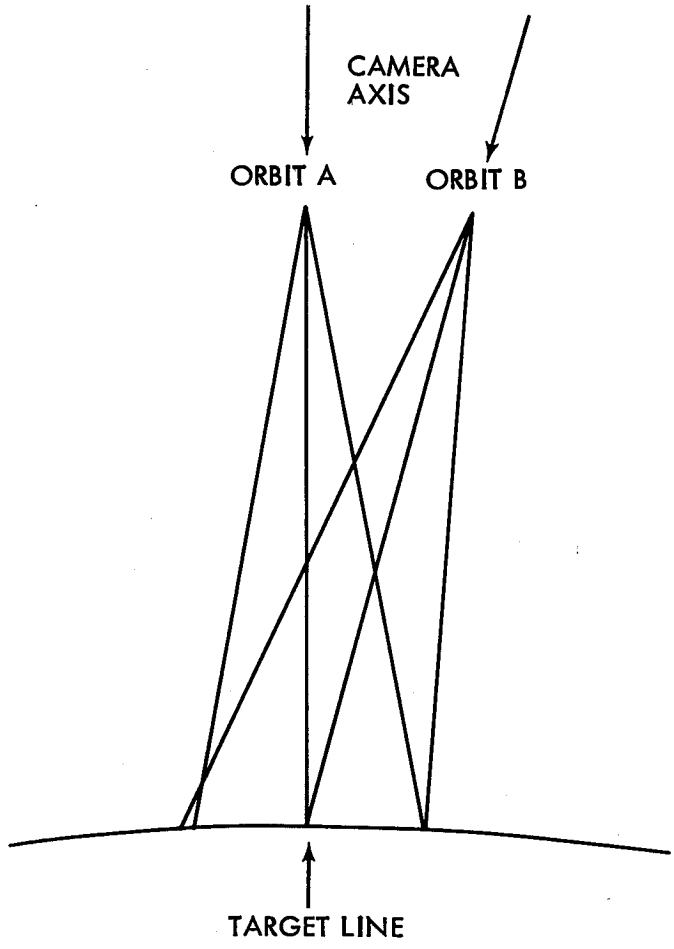

Figure 3-1: Camera Orientation for Convergent Telephoto Stereo

The value of oblique photography in the interpretation of lunar topography was demonstrated initially by the Earth-Moon photograph of Mission I and by a number of additional Mission II photographs. This technique was employed more extensively on Mission III, with 23 of the planned 32 secondary sites photographed with the camera tilted more than 10 degrees.

Deviations from conventional near-vertical photography influence the photographic results with respect to areal coverage, ground resolution, photogrammetric characteristics, and intraframe exposure gradients. The variations in camera pointing do not affect those properties related to the inherent characteristics of the Lunar Orbiter photo subsystem such as processing, readout, and reconstruction. They will, however, influence operation of the V/H sensor and its ability to correct for image motion that will be variable within a frame where the camera axis is tilted.

Mission III photography is characterized, in general, by the highest quality of photography thus far achieved by the Lunar Orbiter program. The unavoidable processing marks (processor-stop lines, Bimat pull-off, and snake-eyes) present in photographs of Missions I and II, and illustrated and described in Volume II of the corresponding mission final reports, were present in Mission III photographs.

No operational or functional failures of the cameras occurred during the mission and all primary and all secondary sites (except one that was deleted for operational reasons) were successfully photographed. Unfortunately, failure of the film advance motor due to a logic disturbance prevented completion of final readout. Final readout of 137 of the 211 dual frames was completed and priority readout resulted in reconstruction of the equivalent of 20 frames not reached in final readout, for a total of 157 dual frames.

3.1.1 Exposure

Compensation for the difference in light transmission between the wide-angle and telephoto lenses was accomplished for Mission III. The installation of a neutral-density filter, having a density of 0.21 ±0.02 on the wide-angle lens, successfully balanced the exposure by the wide-angle lens with that by the telephoto. The exposure differential that was a problem on the first two missions was small (0.1 density) for Mission III and did not present an operational problem or appreciably affect photographic quality.

The observations concerning exposure are based primarily on the evaluation of second-generation, 35-mm GRE positive film copies. Since direct quantitative determination of spacecraft film density is impossible, GRE film offers the next most direct means of evaluating exposure and resolution. Spacecraft film exposure cannot be judged from positive opaque prints because of the image density changes introduced in the production controls of such prints.

Photography of the Moon from lunar orbit presents many problems, one of the more significant being the photometric characteristics of the target area. The primary source of this information is Earth-based observations, which are subject to limitations and errors introduced by the distance that affects resolution or the lunar area over which the sensor integrates the reflected light, and the Earth's atmosphere that affects the light intensity and its spectral characteristics. In addition, one of the most important parameters—albedo—cannot, by definition, be determined by direct observation from Earth, but is derived by extrapolation of a poorly defined data curve.

Accuracy of exposure prediction is sensitive to albedo values and much effort has been given to improve these data by new Earth-based observations by the USGS, evaluation of observations by Shorthill and Saari of Boeing Scientific Research Laboratories, and by evaluation of Lunar Orbiters I and II photography. The results of these efforts are reflected in the change in albedo values used for areas photographed on more than one mission. This comparison is shown in Table 3-1. It is important to note that, in each

Table 3-1: COMPARISON OF SELECTED ALBEDOS OF REPHOTOGRAPHED AREAS

Mission III		Mission II		Mission I	
Site	Albedo	Site	Albedo	Site	Albedo
IIIP-1	0.095	IIP-2	0.088		
IIIP-2	0.097			I-1	0.081
IIIP-4	0.095			I-3	0.075
IIIP-5	0.097	IIP-6	0.087	I-3	0.075
IIIP-7	0.105	IIP-8	0.092	I-5	0.076
IIIP-8	0.102	IIP-11	0.105		
IIIP-9	0.095			I-7	0.076
IIIP-11	0.080			I-8.1	0.069
IIIP-12	0.080			I-9.2	0.068

Table 3-2: FLIGHT FILM EDGE-DATA GRAY SCALE DENSITIES

Step	Log E	Density ASA Visual	Density Readout
1	$\bar{2}.55$	0.36	0.28
2	$\bar{2}.60$	0.37	0.29
3	$\bar{2}.71$	0.39	0.32
4	$\bar{2}.83$	0.42	0.35
5	$\bar{1}.02$	0.49	0.44
6	$\bar{1}.22$	0.65	0.63
7	$\bar{1}.42$	0.87	0.89
8	$\bar{1}.66$	1.17	1.20
9	$\bar{1}.87$	1.45	1.34 (est.)

case, the areas are not exactly duplicated and the variation in albedo within a photographed area will account for part of the differences.

Quantitative determination of spacecraft film density cannot be used as a measure of exposure evaluation since direct measurement is impossible. Determination of spacecraft film density from the edge-data gray scale on the GRE film is difficult because each step in the reconstruction—from spacecraft readout scanning through production of the GRE film record or copy being used—must be considered and evaluated. The edge-data gray scale was calibrated using Bimat-processed flight film during preflight testing at ETR. The density readings are listed in Table 3-2 and the location of each step on the H&D curve is shown in Figure 3-2. Measurements were made with an Ansco Model 4 microdensitometer calibrated for ASA visual density. It should be noted that the H&D curve of Figure 3-2 plots visual densities versus log exposure, rather than readout densities. Equivalent readout densities for the gray scale obtained from the conversion curve shown in Figure 3-3 are listed in Table 3-2.

Changes in premission exposure predictions were made during the course of the mission on the basis of QUAL computer program using data on observational geometry and illumination conditions derived from actual orbital characteristics and target locations. As mission data became available for on-site evaluation of priority readout, this information was used to compensate for any exposure bias that became apparent. Approximately one third of the primary- and secondary-site exposures were changed from those originally planned in order to incorporate the latest information.

Telephoto frames usually display a wider range of image densities than the associated wide-angle frames. Under controlled exposure conditions and uniform flat field illumination, the center of the camera film plane will receive the most light because of the lens characteristics. This inherent effect is more noticeable in the telephoto than in the wide-angle photographs. For some sites, the combination of this effect with overall underexposure often produces very dense positive images in the beginning and end framelets of telephoto frames. The high densities result in some loss of lunar surface detail in such framelets. Where general overexposure occurs, the end framelets of telephoto frames

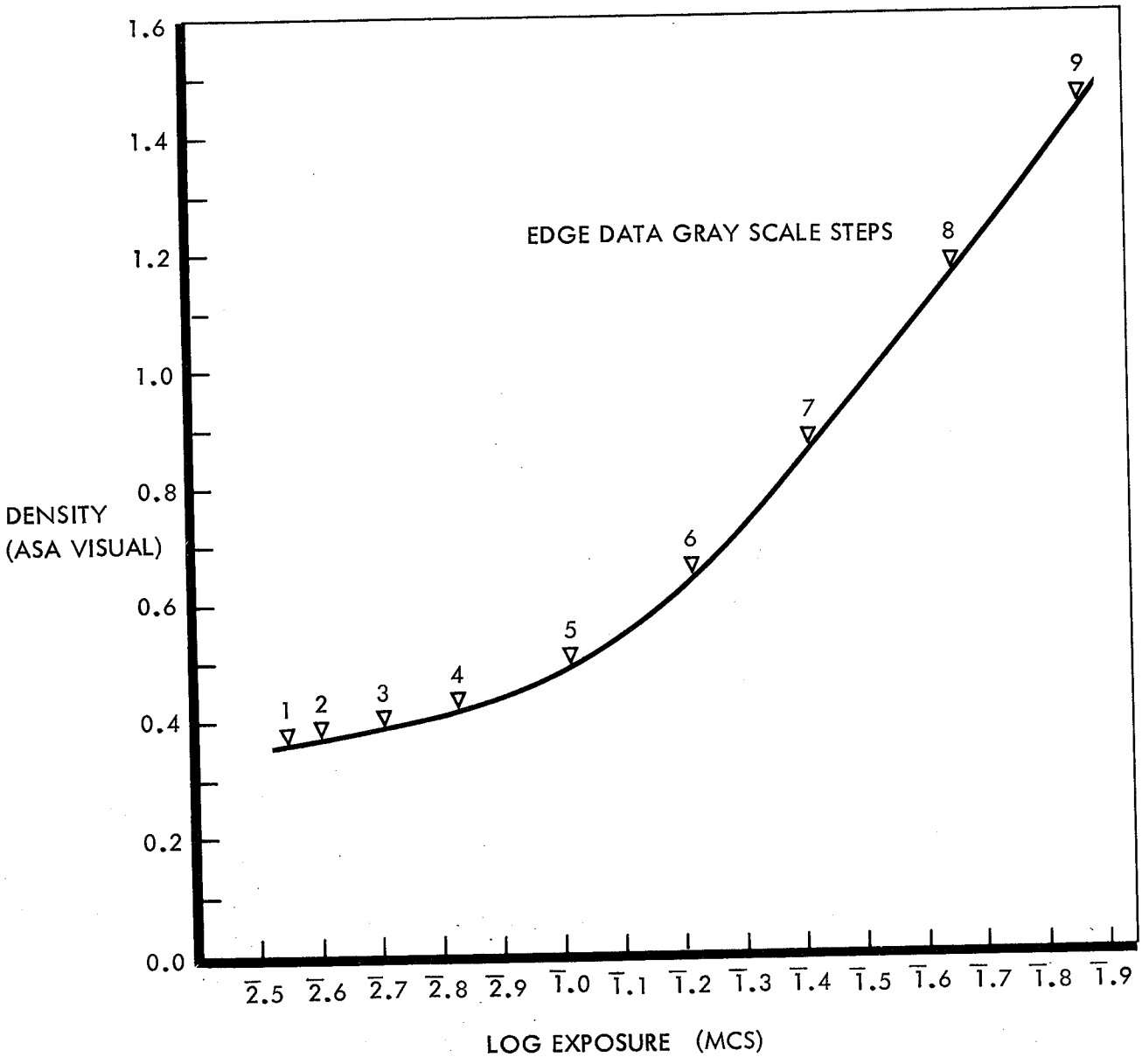

Figure 3-2: Flight Film Gray-Scale Calibration

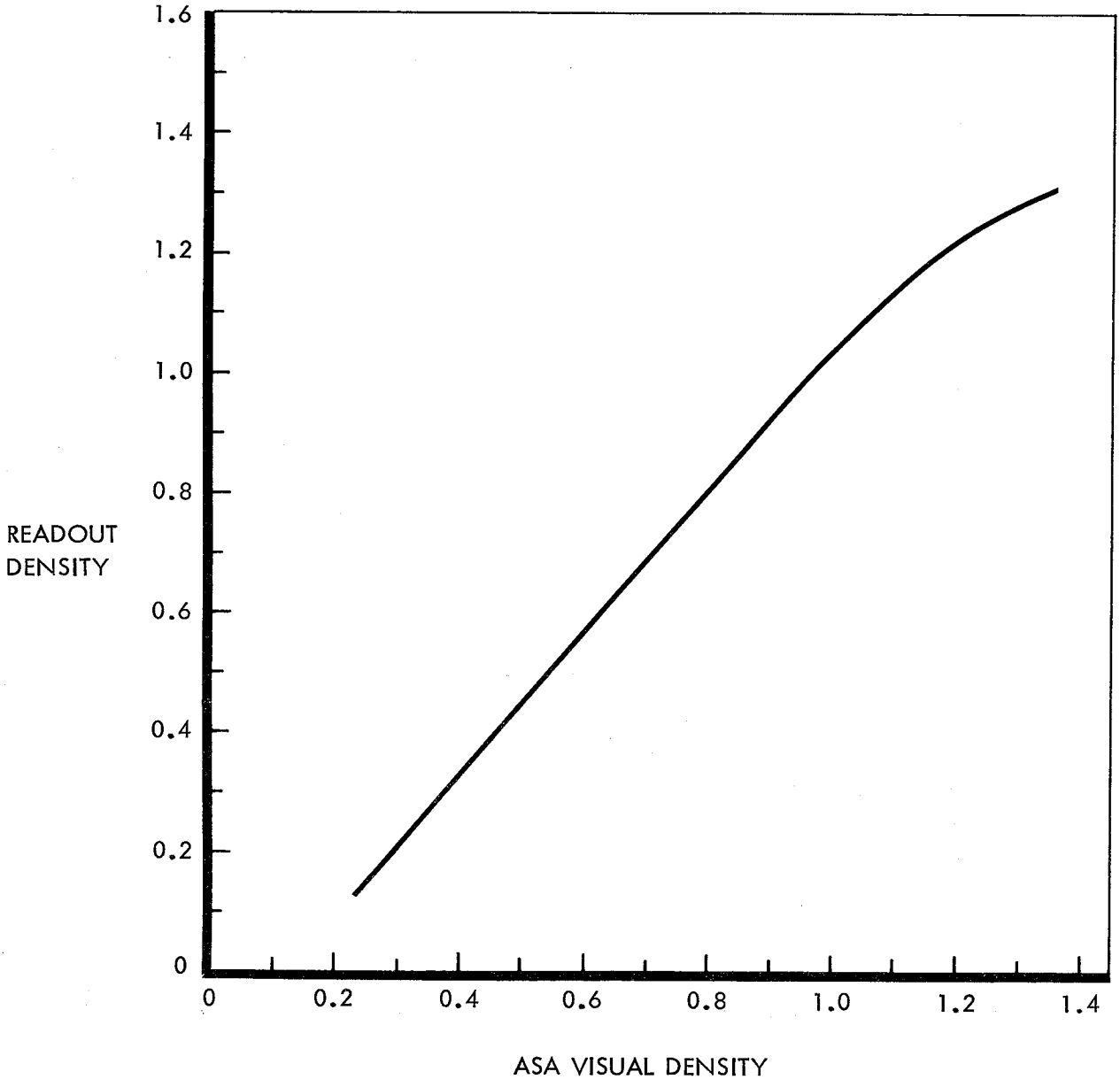

Figure 3-3: A.S.A. Visual vs. Readout Density for Bimat-Processed SO-243

are often of nearly optimum density, but the on-axis framelets have thin, low-density images. Details are often lost in the highlight areas in the latter case.

Photographs of the first six primary sites ranged from slightly to quite underexposed. The exposure of remaining primary-site photographs was generally good, although some variations occurred because of terrain, albedo, and illumination geometry differences. The oblique photography used in some secondary sites imposed a very wide range of scene brightness values. Very satisfactory secondary-site photos were obtained even though the scene luminance range often exceeded the design limits of the photographic subsystem and its associated subsystems. However, the latitude of the system made it possible to obtain good photographs even when considerable underexposure or overexposure occurred within limited areas of the frames.

3.1.2 Resolution

The design specifications for resolution by the telephoto lens require detection, from a nominal altitude of 46 km, and with a peak-to-peak signal-to-RMS-noise ratio of 3:1, of a 2-meter base, 0.5-meter high cone and a 7- by 7-meter flat area having a slope of 7 degrees providing maximum contrast. Although the target models specified provided a reasonable representation of surface features of concern useful for design, such precisely known targets do not exist on the Moon. Determination of resolution, at the stated signal-to-noise ratio, of the actual mission photographs must be accomplished by means other than simply measuring lunar surface image detail. Further, to obtain a value statistically significant, a large number of measurements would be necessary.

A means was sought for estimating image resolution, by visual examination of the GRE record, that might provide a useful comparison. Such a method was not intended to substitute for precise quantitative measure of specification compliance.

It was found that the scan lines provide a convenient unit of measure of image resolution. This criterion is independent of spacecraft altitude at the time of photography, as opposed to ground measure, and is also independent of copying processes that might alter the scale of the film being examined. For these reasons, resolution has been estimated and reported in the following discussions largely in this manner.

The resolution requirement for Lunar Orbiter photography has been stated as that necessary to detect a 1-meter object with the telephoto lens and an 8-meter object with the wide-angle lens from an altitude of 46 kilometers. This requires a resolution of 76 lines per millimeter on the spacecraft film or 10 lines per millimeter on the 35-mm GRE reconstructed record. There are approximately 40 scan lines per millimeter on the GRE record. Thus, the resolution requirement is equivalent to detection of objects whose images span four scan lines.

Since ground resolution is directly proportional to the spacecraft altitude (or slant distance), it is related to scan lines by the expression:

$$\text{Ground resolution in meters} = \frac{N}{4} \times \frac{H}{46}$$

where N is the number of scan lines spanned by the smallest objects detected, and H is the spacecraft altitude in kilometers. (This applies to the telephoto coverage; wide-angle resolution must be increased by a factor of 8.)

It was found that the resolution requirements appeared to meet or slightly exceed system requirements for the detection of 1-meter features in telephoto frames and 8-meter features in wide-angle frames, on-axis, from a nominal altitude of 46 km. This estimate is based upon visual examination of a 35-mm second-generation copy of the GRE film under magnification sufficient to distinguish scan lines clearly (15 to 30x). Since the examination was visual, the requirement for detection at a signal-to-noise ratio of 3:1 could not be established by quantitative means.

Resolution is somewhat dependent upon variables encountered in photography at each site, such as target characteristics, illumination, exposure, etc. Therefore, this characteristic will be included in the discussion of the individual sites.

3.1.3 Processing

Processing marks that are the result of the intermittent processing schedule required by mission design were present as in Missions I and II. These include the Bimat pull-off and processor-stop lines, and the "snake-eyes." Also present were the diffuse light lines running longitudinally on the spacecraft film. The source of these lines was not established in time to make the necessary corrections for Mission III.

The small-scale noise pattern, described previously in the Lunar Orbiter Mission I Final Report, Volume II, was present throughout the reconstructed record. Although studies have been made in an attempt to determine the cause of the noise pattern, positive identification has not been successful and thus no corrective action has been possible. The presence of the noise pattern is significant since it appears to be the limiting factor in system resolution. The size of the pattern is such that it corresponds closely to the resolution requirement, and differentiation between small surface features or texture and the noise is frequently difficult. With experience, and by close attention to illumination characteristics, detection of small surface detail becomes more reliable.

The blemishes referred to as "lace" appear occasionally throughout the mission photography. Its appearance is random and variable in extent. The cause of this defect has not been found. Examination of photographic prints representing nearly all of the mission photography has indicated that this type of blemish may be less extensive than on the previous missions, although a quantitative measure was not attempted because of time limitations.

3.1.3.1 Discussion of Defects

Processor Stop Line—This line normally is less than 0.5 framelet wide and crosses the film at an angle of 90 degrees to the direction of film motion. The Bimat stop line is caused by the pressure differential at the lamination point of the film and the Bimat. This pressure differential and possible dryout effects result in displacement of the Bimat emulsion and cause improper or no processing. The Bimat stop line is usually closely followed by two lesser defect lines parallel to the stop line. These lines, approximately six and ten framelets away, are due to pressure at the tangent points of the Bimat contact on the first roller prior to lamination. The emulsion side of the Bimat contacts this roller for about an 80-degree wrap. Two other rollers contact the emulsion side of the Bimat in the same manner; however, corresponding defects have not been observed, no doubt due to the decreasing Bimat tension in this area. These lines are associated with the location of the Bimat at the start of each processing-on period and can be predicted following location of the first Bimat stop line during readout. There is no operating technique that would prevent this condition other than continuous processing.

Bimat Pull-Off Line—This line generally appears as a curved line that crosses the entire Bimat processed area. It normally starts at a slope of roughly 15 degrees off right angles to the film and then terminates as a curve. The Bimat pull-off line is often associated with a partial line of defective processing spots. This combination of lines is normally located on the film about 11 inches following the Bimat stop line. The Bimat pull-off line appears to be related to the variances in adhesion between the emulsion and the backside of the Bimat as it just starts to pull away from the Bimat wraps on the supply spool. The location of this defect is subject to some variation due to variation in Bimat unrolling tensions and to the changing diameter at the roll as Bimat is used. No known method of eliminating this defect is known.

"Snake Eyes"—These appear as two oval-

shaped spots near the center of the film. They are generally spaced about 0.375 inch apart, are associated with the location of the Bimat stop line, and follow it by about 4.2 inches. Pressure of the Bimat cut encoder roller on the back of the Bimat forces the emulsion against the cutout area edges of the conductivity roller during the processor-off time. Because the size and degradation of this condition seems to vary with processor-off time, no known solution is available other than continuous processing. This condition does not always appear following a processor-off period.

Longitudinal Lines—Two, three, or four longitudinal lines of varying density are present at times on the film. Tests have been made to determine the cause of the streaks. It was found that, as the film passed into the camera storage looper, a static charge was generated when the film rubbed against the first teflon separator in the looper end. The streaks were caused by static discharge onto the film, which produced localized fogging.

"Freckles" or "Queen Anne's Lace"—This appears as a spotted area of unprocessed film arranged in a random manner. The areas vary in size and location on the film and do not follow any repeating pattern. No known reason for these defects has been found; they could be attributed to bubbles in the Bimat, an unknown reaction of an area of the Bimat, or processing characteristics when the tension of the film and Bimat is varied due to the frequent starting and stopping of the processor-dryer. At present there is no known way to prevent this condition.

3.1.3.2 Avoidance of Processing Defects in "High-Value" Frames

There are no known changes to present operating techniques that will reduce the number of defects when the mission is programmed with photos and processing spread out through so many orbits.

- Freckles or lace appearance cannot be predicted.
- The quality of processing has not shown degradation at the end of the processing period; therefore, it is believed that no improvement would be possible by shortening the time to completion of processing.
- Priority readout to the extent used in Mission III does not seem to affect processing quality.
- The practice of processing at least two frames every 4 hours or each orbit as a minimum is still recommended. Fewer defects would be present if more frames were processed at one time.

3.1.4 Readout and Reconstruction

Readout of the photographs was of very good quality. However, problems were encountered with the readout film advance mechanism that occasionally resulted in a frame-let being scanned more than once, or the film was not advanced the exact specified amount. Where no film advance occurred following scan of a framelet, it was rescanned; the repetitive framelets were identical on the reconstructed image. Where film advance was less than the required 2.54 mm, the image on adjacent framelets overlaps more than the nominal 0.16 mm (1.2 mm on the reconstructed record). With normal reassembly techniques, such excess overlap results in strips in which the image is duplicated. During final readout, a failure occurred that prevented readout of frames below Telephoto Frame 79. During priority readout, portions of 36 telephoto pictures—equivalent to 14 full frames, and 19 complete and three partial wide-angle photographs that were not reached during final readout—were acquired. This is diagrammed in Figure 3-4.

A more detailed discussion of the readout drive malfunction and of the failure that terminated final readout is included in Volume III.

Image distortion introduced by nonlinearity of the optical-mechanical scanner was present, but inclusion of the pre-exposed reseau mark pattern allows corrections to be made to metrical measurements on the photo-

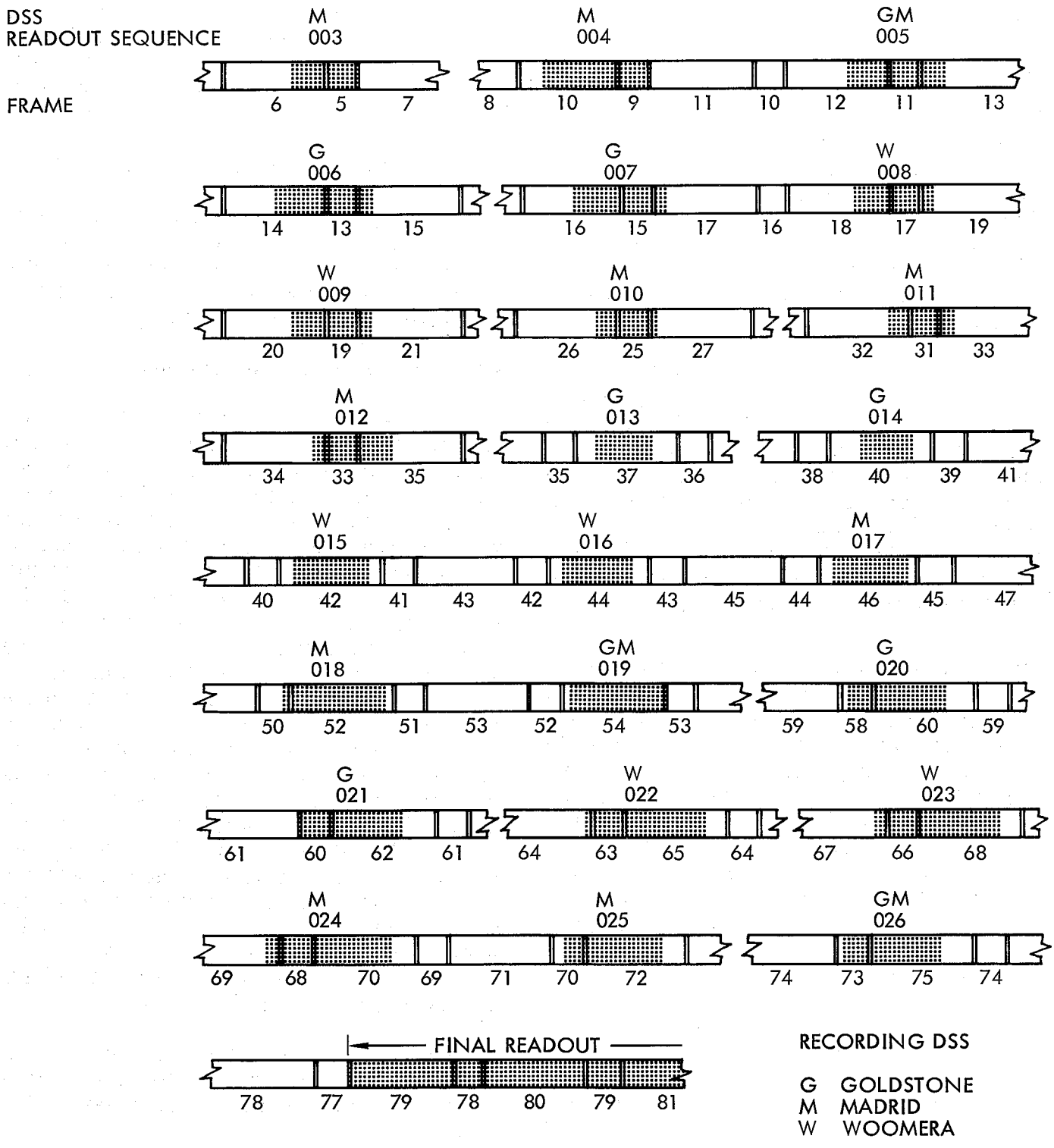

Figure 3-4: Mission III Priority Readout

graphs. The reseau pattern used for Mission III is illustrated in Figure 1-1. The newer pattern, having 23 marks arranged in two lines per framelet instead of a single nine-mark pattern used on Mission II, provides a means for more detailed and more reliable distortion detection and correction.

The characteristics of the spacecraft readout are such that a video signal variation across the width of a framelet, not related to the photographic image, is introduced. The amount and character of the variation, appearing as a low-profile "W" form on the GRE A-scope, are dependent upon focus adjustment of the line-scan tube. The result is a density variation across the width of the reconstructed framelet that has been described as "tiger stripes" in the reassembled photograph. A technique that greatly reduces this effect in GRE reconstructions made from tape recordings of the video signal has been developed by Boeing and is in use at the Langley Research Center. Basically, the signal variation, or "signature," for a readout sequence is determined at intervals across the framelet width. Either 20 sections evenly spaced, or 16 with an additional eight subdivisions distributed near either end of the scan line where the variation is most evident, may be used. A proportional compensating signal, as established by the signature, is applied to the GRE input at the appropriate position during the scan of each line. By very careful adjustment of the equipment, the established periodic variation can be reduced markedly. The technique significantly enhances the photographs for visual interpretation. The stepwise character of the correction, although not detectable visually, may introduce some error in precise photometric measurements.

3.1.5 Reassembly

The reassembly of photographs of both Missions II and III was similar. Paper prints were prepared by NASA, Langley Research Center, and the Army Map Service. Hand-reassembled GRE records generated from the FR-900 video tape record were used by NASA. The Army Map Service used GRE film copies, made by Eastman Kodak, in their production of prints. Machine reassembly was done by Eastman Kodak Company at Rochester, New York, but paper prints were not made by them from the reassembled negatives.

3.2 PRIMARY-SITE PHOTOGRAPHY

Three basic procedures were used in photographing primary sites with the exception of Sites IIIP-9 and IIIP-12 for which special procedures were established. The basic procedures used were:

- Vertical* photography on the orbit that passes nearest to the site. The specified site coordinates may not be within the telephoto coverage.
- The camera pointed at the site from the nearest orbit, using cross-track tilt of the camera axis if necessary.
- Telephoto convergent stereo by photography on successive orbits. Cross-track tilt used to point camera at site with one pass vertical or using cross-track tilt necessary from nearest orbit.

*"Vertical" assumes attitude errors and effect of surface curvature. Actual camera is near-vertical.

The special procedures used at Sites IIIP-9 and IIIP-12 are described in the discussion of these individual sites, Sections 3.2.9 and 3.2.12, respectively.

The photographic parameters for the primary sites are summarized in Table 3-3.

Photographic evaluation of primary and secondary sites photographed with the first 78 frames was based only upon the limited priority readout. The evaluation of Primary Sites IIIP-1 through IIIP-6 could not, therefore, consider complete site photography, and is necessarily incomplete and not considered to be adequately representative of some sites. A diagram showing the photographs that were read out and reconstructed is presented for each of these primary sites. In each case, the area photographed is represented with

the frames or portions of frames read out outlined by a solid line and with the frame number shown.

The photographed area for each primary site is also shown plotted according to the corner coordinates computed by the EVAL program using postmission data where available. Where insufficient data was available, because of limited data for the first six sites, the planned coverage is plotted. The position of the specified target is shown. It will be noted that the target position is not precisely centered within the coverage area of sites following Site IIIP-6. The apparent offset is the result of a combination of data uncertainties and errors. These include:

- Camera-on Time
  The commanded camera-on time is computed on the basis of orbit prediction for only the first exposure of a sequence. Subsequent exposure intervals are determined by the velocity-to-height ratio.

Table 3-3: PHOTOGRAPHIC PARAMETERS FOR MISSION III PRIMARY SITES

Site	Location		Phase Angle (deg)	Selected Albedo	Incident Sun Angle	Shutter (sec)	Altitude Range (km)	Frame Numbers
	Long.	Lat.						
IIIP-1	35°15′E	2°55′N	74.8	0.095	75.7	0.04	55.8 - 53.5	5 - 20
IIIP-2a	42°25′E	0°50′S	65.8	0.097	66.7	0.02	50.9 - 51.3	25 - 32
IIIP-2b	42°41′E	0°55′S	73.3	0.097	64.6	0.02	51.6 - 51.8	33 - 36
IIIP-3	20°15′E	3°20′N	73.7	0.092	80.1	0.04	59.3 - 56.4	40 - 43
IIIP-4	27°27′E	0°37′N	72.3	0.095	71.0	0.02	48.9 - 48.7	44 - 51
IIIP-5a	24°31′E	0°27′N	67.8	0.097	72.2	0.02	48.8 - 48.5	52 - 59
IIIP-5b	24°31′E	0°27′N	74.5	0.097	70.4	0.02	48.0 - 47.9	60 - 67
IIIP-6	21°30′E	0°20′N	69.3	0.096	71.5	0.02	48.0 - 47.6	68 - 71
IIIP-7a	1°17′W	1°02′N	69.4	0.105	76.9	0.04	47.8 - 47.0	86 - 93
IIIP-7b	1°20′W	0°55′N	71.6	0.105	75.0	0.04	46.5 - 46.0	94 - 101
IIIP-8	19°50′W	0°50′S	72.3	0.102	72.4	0.04	45.4 - 45.3	124 - 131
IIIP-9a	23°11′W	3°09′S	62.3	0.095	70.0	0.02	46.4 - 46.7	137 - 144
IIIP-9b	23°11′W	3°09′S	66.3	0.095	68.5	0.04	47.4 - 47.9	145 - 152
IIIP-9c	23°11′W	3°09′S	68.5	0.095	67.0	0.04	48.5 - 49.2	153 - 160
IIIP-10	42°00′W	1°45′N	84.5	0.080	79.0	0.04	52.3 - 51.3	163 - 170
IIIP-11	36°56′W	3°17′S	67.9	0.080	68.4	0.04	51.2 - 51.9	173 - 180
IIIP-12b.2	43°52′W	2°23′S	67.6	0.080	73.1	0.04	50.5 - 50.5	181 - 184
IIIP-12a			68.2	0.080	71.9	0.04	50.9 - 50.5	185 - 200
IIIP-12b.1			68.7	0.080	69.7	0.04	51.8 - 52.1	201 - 204
IIIP-12c			82.3	0.080	68.9	0.04	52.1 - 52.8	205 - 212

- Orbit Prediction
  Orbit parameters are based on the current models of the lunar gravitational field. Significant uncertainties exist in these models.
- Spacecraft Attitude
  The spacecraft attitude, and thus the camera axis, is subject to a point error and to the ±0.2-degree deadband in control. In addition, where cross-track tilt was used for a sequence, the coverage area is more or less distorted and the principal point will not coincide with the center of the area photographed.
- Uncertainties in Spacecraft Altitude
- Chart Accuracy
  The ACIC lunar charts (LAC and AIC) are subject to errors arising from limitations imposed by Earth-based observation. Uncertainties indicated on the Reliability Chart of the AIC chart series is variable, but in general is greater toward the limb.
- Selenodesy
  Selenographic coordinates given for frame corners are computed from orbital parameters; the chart coordinates are determined from Earth-based observation. Thus, the comparison involves coordinates derived by two completely different techniques.

Some of these errors or error sources are discussed in more detail in Section 4.2. Time limitations have prevented any extensive effort to compare actual photographic coverage with the computed or with the planned coverage by matching photographs with the charts. For this reason, "actual" coverage of each site has not been indicated on the site coverage plots.

3.2.1 Site IIIP-1

Primary Site IIIP-1 is located at 35°15′E, 2°55′N in the southeastern portion of Mare Tranquillitatis. The site was planned to provide telephoto coverage of smooth terrain along the northeastern margin of Mission II Site IIP-2 and a small outcrop of dark mare to the east that appears smooth in Wide-Angle Frame 48 of Mission I. The site includes dark mare and a broad, low dome south of Maskelyne F. Crater concentration is abnormally low.

The site was photographed by a sequence of 16 frames exposed in the fast mode with a shutter speed of 0.04 second. The inflight prediction of coverage is shown in Figure 3-5. The frames read out in priority mode are diagrammed in Figure 3-6.

The photographs show no sharply defined major topographic features, but rather, low-profile topography with gentle slopes that did not impose a severe luminance range. In some wide-angle frames, a luminance range across the frame, decreasing in the direction of flight, is apparent. However, average scene luminance appeared to be slightly less than optimum and, in darker areas, the low light levels tended to be below system design limits.

The wide-angle and telephoto frames obtained in priority readout were of generally good photographic quality although some differences occurred. All telephoto frames and some wide-angle frames read out appeared to be slightly underexposed. Despite the greater image densities resulting from less-than-optimum scene luminance, on-axis resolution of the telephoto frames appears to be satisfactory. Craters spanning as few as three to four scan lines could be detected in the middle on-axis framelets of the 610-mm photos examined.

As expected, because of lens characteristics, detection of small lunar features was more difficult in off-axis framelets.

The wide-angle photos examined appeared to have a more desirable average image density than the telephotos. This resulted in more nearly optimum image characteristics and resolution. Craters spanning as few as three scan lines could be identified. In some frames, rocks or projections spanning two or three scan lines were observed.

Although slightly more exposure would have been desirable for this site, the 0.04-second

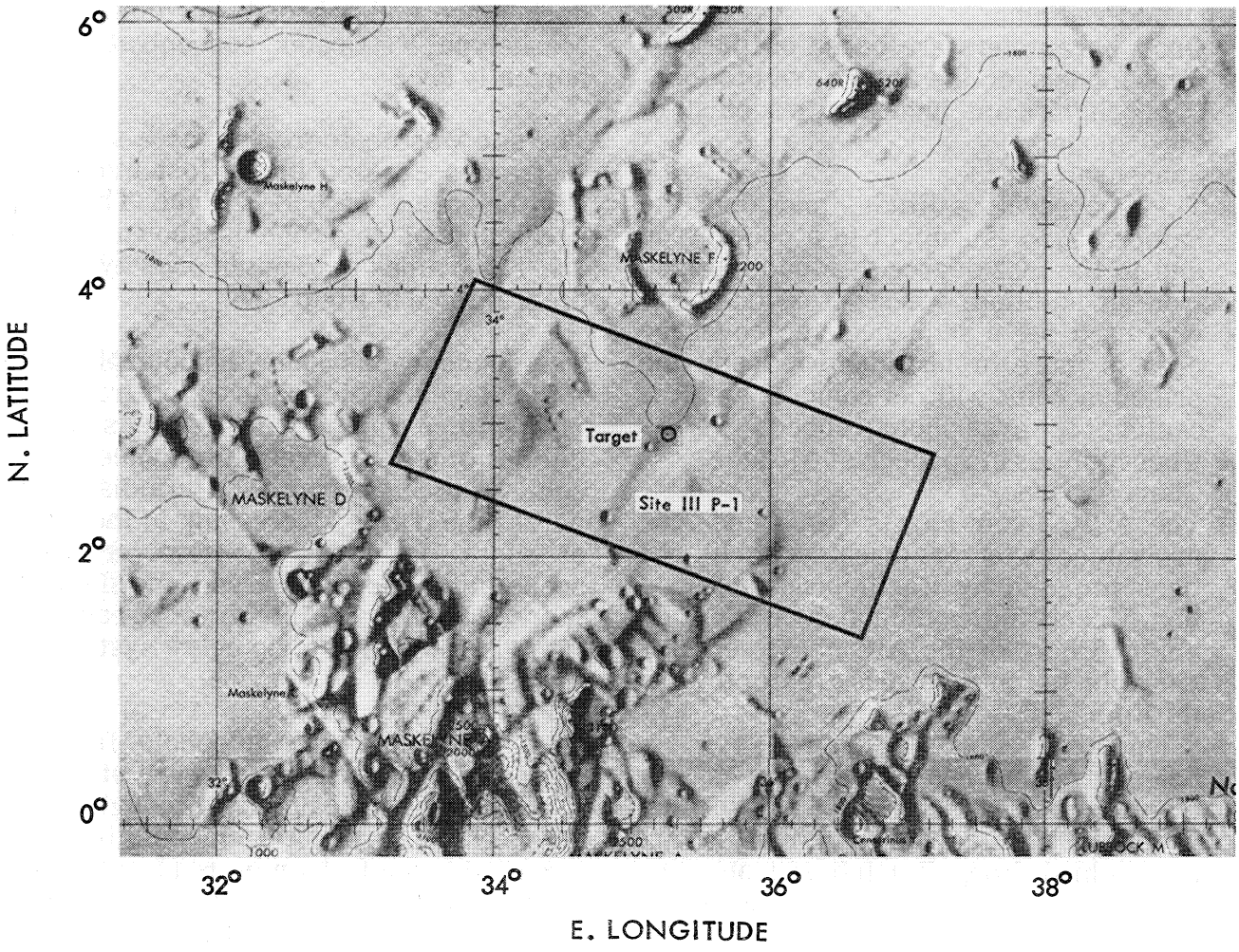

Figure 3-5: Coverage of Site IIIP-1; Inflight Prediction EVAL Computation

shutter speed actually used provided the maximum available in the photographic subsystem.

During the "command conference" prior to photography of Site IIIP-1, a decision, based upon predicted exposure requirements, was made by SPAC to change shutter speed for Site IIIS-1 to 0.02 second rather than use 0.04 second planned for both IIIP-1 and IIIS-1. The change in shutter speed was to be made by real-time command following photography of site IIIP-1. Because of the short time interval between completion of the first sequence and initiation of the second, there remained about two minutes in which to execute the real-time shutter-speed change. The sequence of commands used to effect the SPAC directive, together with the internal logic of the spacecraft programmer, prevented the time codes from functioning for Site IIIP-1 exposures. Because the time code provides the only precise time-of-exposure data for each frame, postmission EVAL computa-

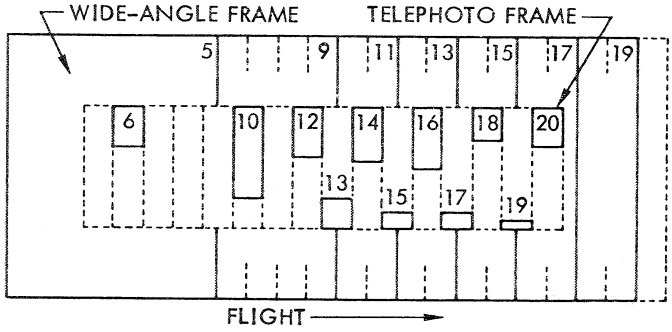

Note: Solid line outlines frames (or portions) read out. Dashed lines outline frames photographed but not read out.

Figure 3-6: Priority Readout of Site IIIP-1

tions could not be carried out. To provide the basic information on these frames, the data from the site prediction EVAL is shown for Site IIIP-1 in the table of supporting data (Table 4-8). It should be noted that the listed frame corner coordinates are less reliable than for other sites because of the time uncertainty.

3.2.2 Site IIIP-2

Site IIIP-2 was scheduled to be photographed by two sequences on successive orbits. IIIP-2a location was designated as 42°25′E, 0°50′S, to be photographed with a sequence of eight frames, as shown in Figure 3-7. Site IIIP-2b was located at 42°41′E, 0°55′S, to be photographed by a sequence of four frames. Both sequences were taken in the fast mode with a shutter speed of 0.02 second.

The four frames of the second pass were taken to provide high-resolution, convergent stereo coverage. Because only the priority readout was obtained, telephoto stereo was not recovered. The photographs read out in priority mode are diagrammed in Figure 3-8. This diagram is not intended to represent areal coverage of the site photography since coverage of IIIP-2a and IIIP-2b overlapped.

Site IIIP-2 is located at the western edge of Mare Fecunditatis and includes a portion of the upland terrain separating Mare Fecunditatis and Mare Tranquillitatis. The site lies almost entirely within the area of Mission I Site I-1.

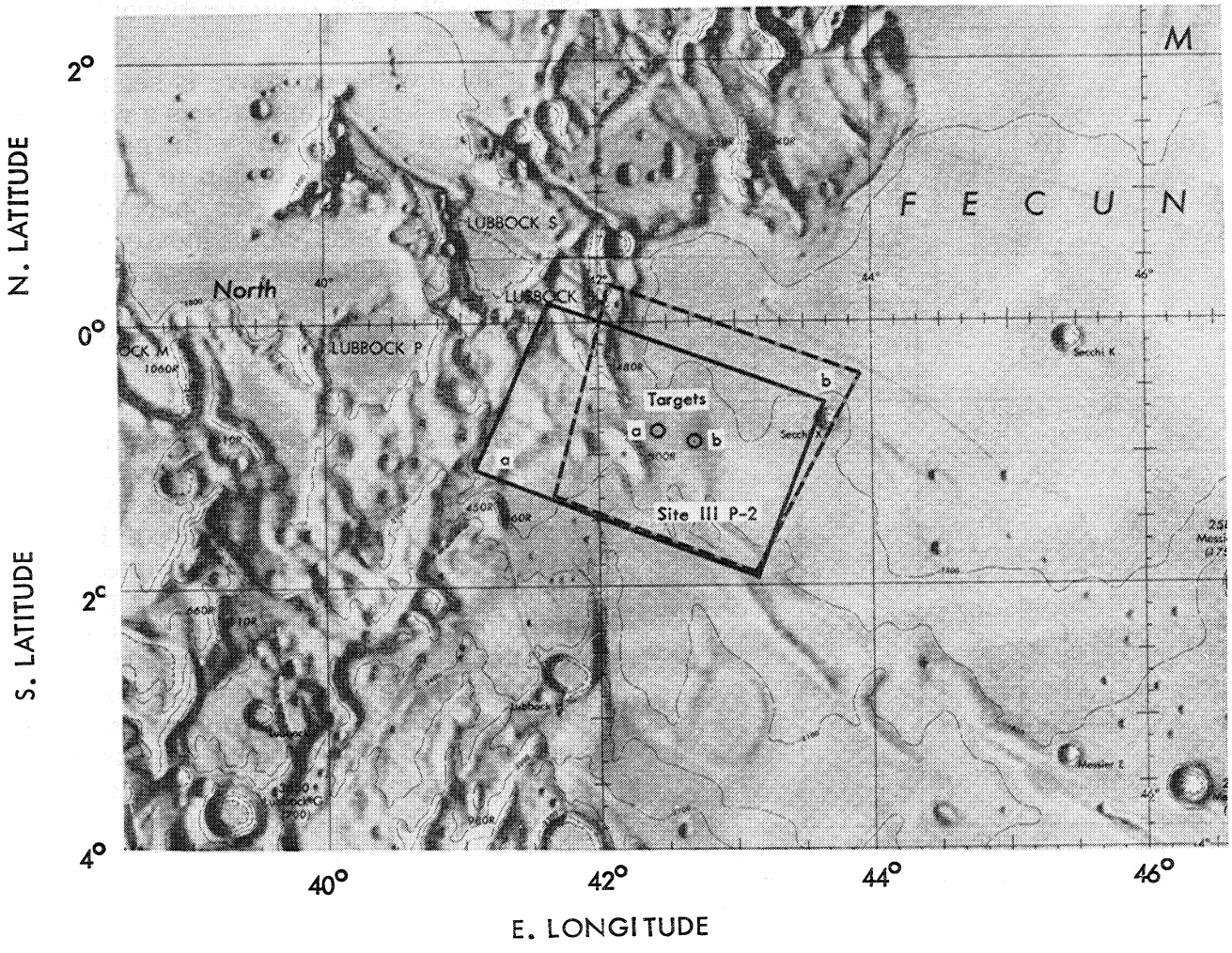

Figure 3-7: Coverage of Site IIIP-2; Inflight Prediction EVAL Computation

Evaluation of photography for this site was limited to the relatively small amount of coverage obtained by priority readout. As indicated by Figure 3-8, three of the wide-angle frames and parts of five of the telephoto frames were read out and reconstructed. Examination of these photographs indicates that they are underexposed or slightly underexposed. Despite the denser images, as seen on film positives, craters spanning as few as three scan lines can be detected in the central parts of the wide-angle frames. On-axis resolution for the telephoto frames cannot be established since no center sections were included in the partial readouts received from the spacecraft. Some detail is lost in the end framelets of the telephoto frames because of high image densities.

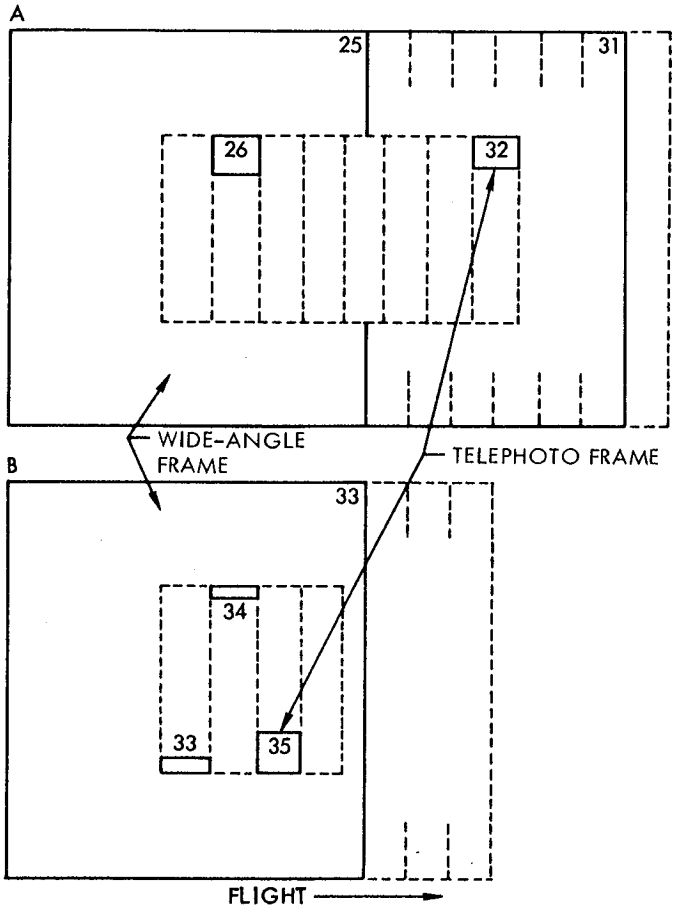

Note: Solid line outlines frames (or portions) readout. Dashed lines outline frames photographed but not readout.

Figure 3-8: Priority Readout of Site IIIP-2

3.2.3 Site IIIP-3

This site was located at 20°15′E, 3°20′N, as shown in Figure 3-9. The area is a relatively smooth mare area between the craters Ritter and Manners. A large, shallow rille runs across the area. Arago B and a portion of Ritter D were included in the area photographed.

Of the four dual frames exposed at this site, the photographs read out in priority mode were most of Telephoto Frames 40 and 42, as diagrammed in Figure 3-10. Frame 42 shows a part of a large crater, probably Arago B, since the charts to not indicate the presence of any other comparable crater in the immediate vicinity. If this is correct, it indicates that the area photographed is only very slightly downtrack from the planned area.

The rille mentioned above is seen in Frame 40 (Figure 3-11). It appears as a very shallow longitudinal formation with gentle slopes generally not steep enough to produce hard shadow. The large crater, part of which is included in Frame 42, is mostly in shadow and shows no detail. The opposite sunlighted interior is overexposed because of the high luminance. The more nearly level areas, however, show good detail.

The two telephoto frames appear to be of good photographic quality although the high average image densities indicate that considerable underexposure occurred. Resolution in the central areas of the frames is satisfactory. Craters and rock-like projections spanning only three or four scan lines can be detected. Definition and contrast are good although the average densities are high on positive GRE film. The minimum available shutter speed of 0.04 second was used for the slow four-frame sequence executed for this site.

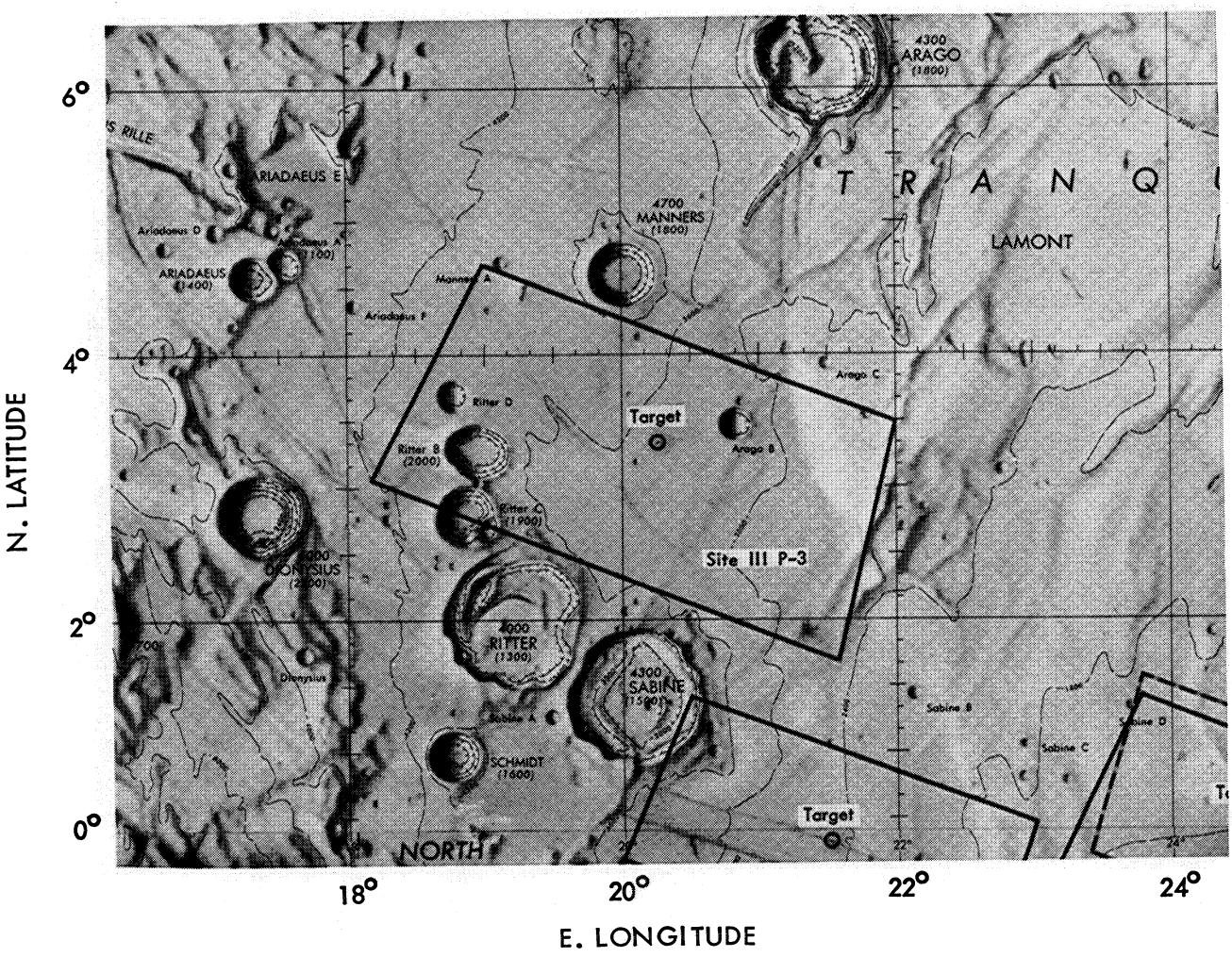

Figure 3-9: Coverage of Site IIIP-3; Inflight Prediction EVAL Computation

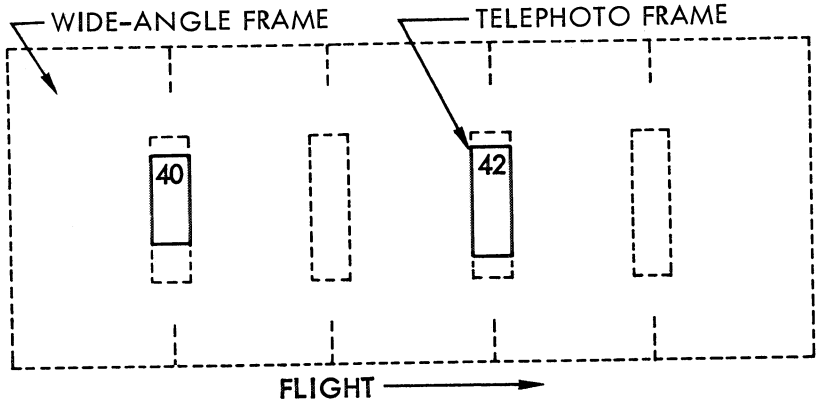

Note: Solid line outlines frames (or portions) readout.
Dashed lines outline frames photographed but not readout.

Figure 3-10: Priority Readout of Site IIIP-3

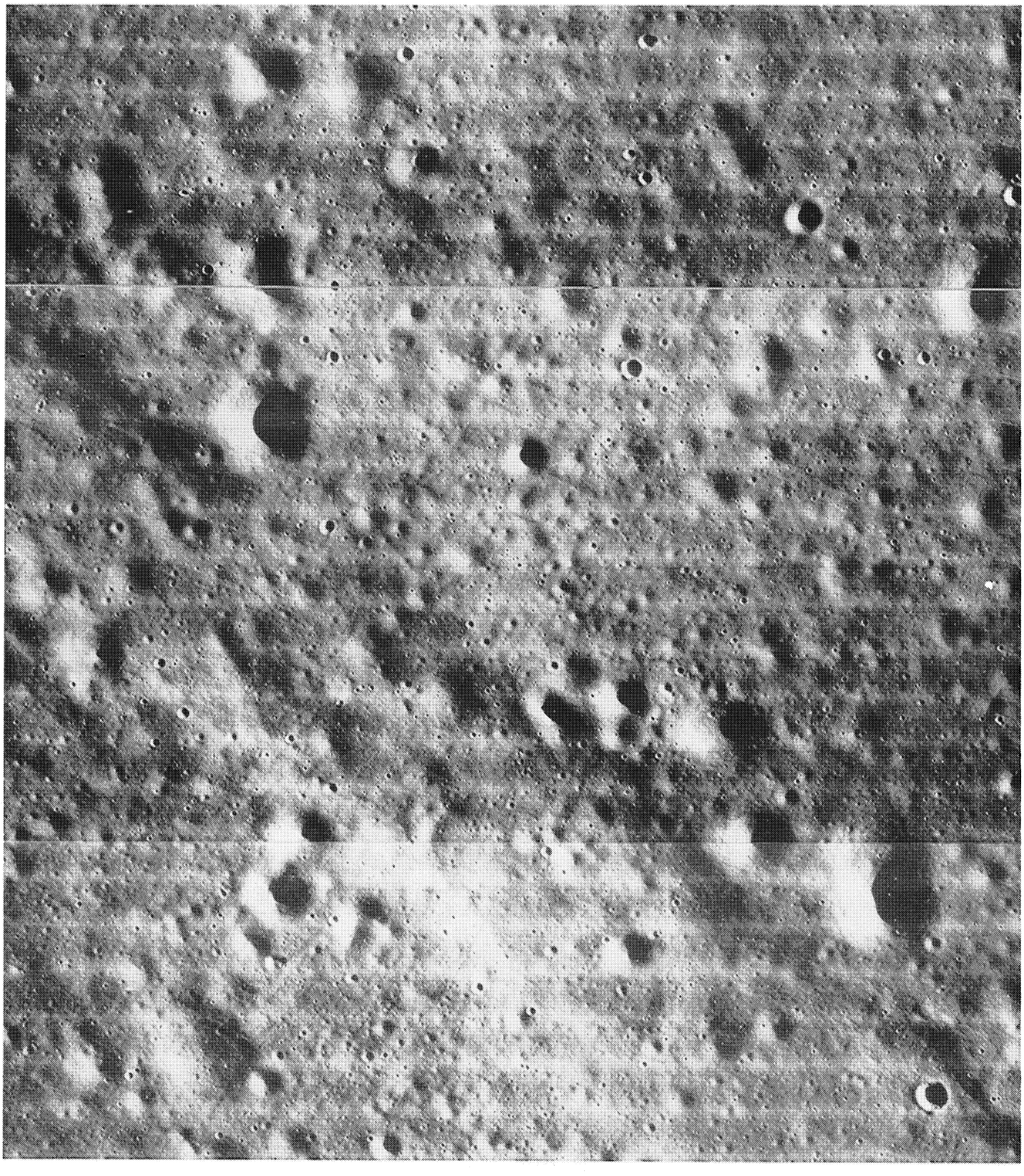

Figure 3-11: Portion of Telephoto Frame 40. Site IIIP-3

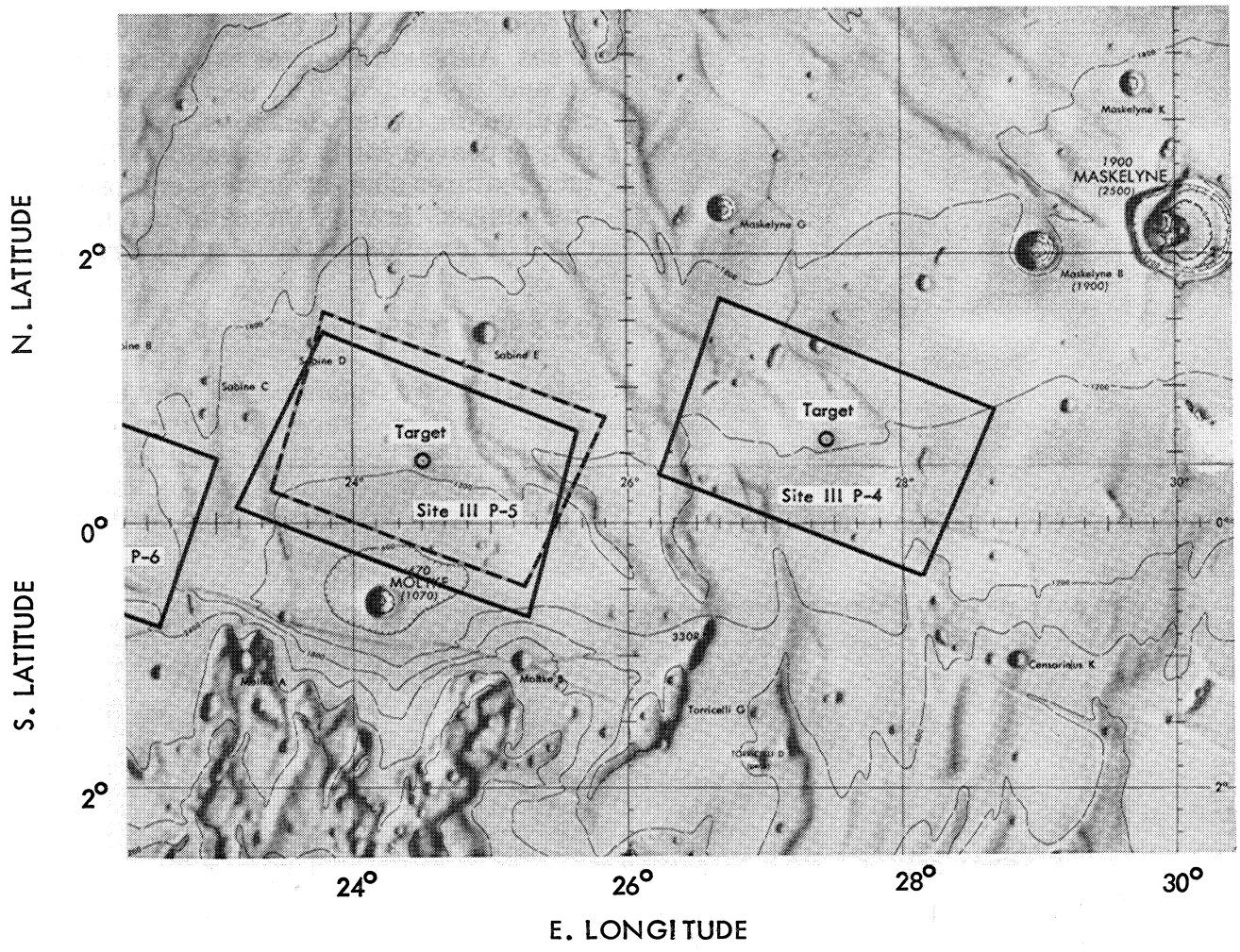

Figure 3-12: Coverage of Site IIIP-4; Inflight Prediction EVAL Computation

3.2.4 Site IIIP-4

Site IIIP-4 location was specified as 27°27′E, 0°37′N, to be photographed from the nearest orbit (Orbit 51) with cross-track tilt of the camera axis as required. The area is located within a mare area southwest of Maskelyne, as shown in Figure 3-12. The area contains low ridges of gentle slope, numerous crater-chains and coalescing craters, and the sinuous rille Rima Maskelyne I. The area is covered by ray systems, presumably originating from the major nearby craters, primarily Theophilus, which accounts for the rather high albedo (0.095) for a mare area.

The area was photographed by a sequence of eight frames taken in the fast mode with a shutter speed of 0.02 second. These photographs were not included in final readout, thus only those read out in priority mode were recovered. The frames read out are diagrammed in Figure 3-13.

The two partial telephoto frames read out for Site IIIP-4 included the center framelets but not all the end framelets. Priority readout also included one end framelet of Wide-Angle Frame 50. Average luminance for this site appeared to be somewhat less than expected for the conditions existing at the time of photography. As seen on positives, such as GRE film, these photographs have relatively high average image densities, with

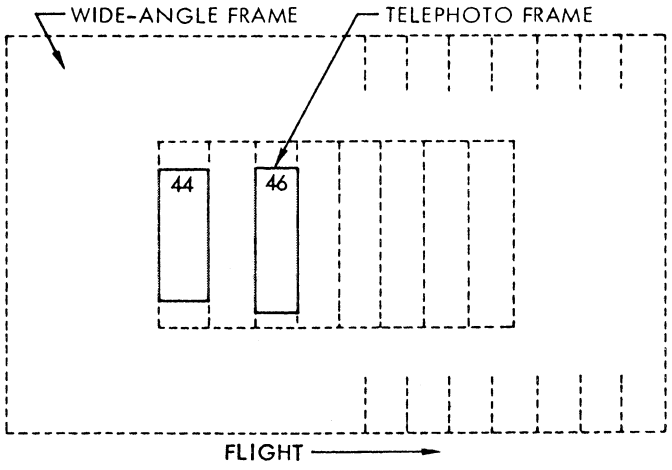

Note: Solid line outlines frames (or portions) readout.
Dashed lines outline frames photographed but not readout.

Figure 3-13: Priority Readout of Site IIIP-4

a considerable loss of detail in the shadow areas. Although a longer exposure time—0.04 second instead of 0.02 second—would have resulted in better densities, on-axis resolution appeared fairly satisfactory. Lunar surface features such as craters and projections spanning as few as three to four scan lines could be observed in the telephoto frames.

3.2.5 Sites IIIP-5a and IIIP-5b

Site IIIP-5 was planned for convergent telephoto stereo coverage of the area as shown in Figure 3-14. The location specified was 24°31′ E, 0°27′N. Two eight-frame sequences were exposed with a shutter speed at 0.02 second

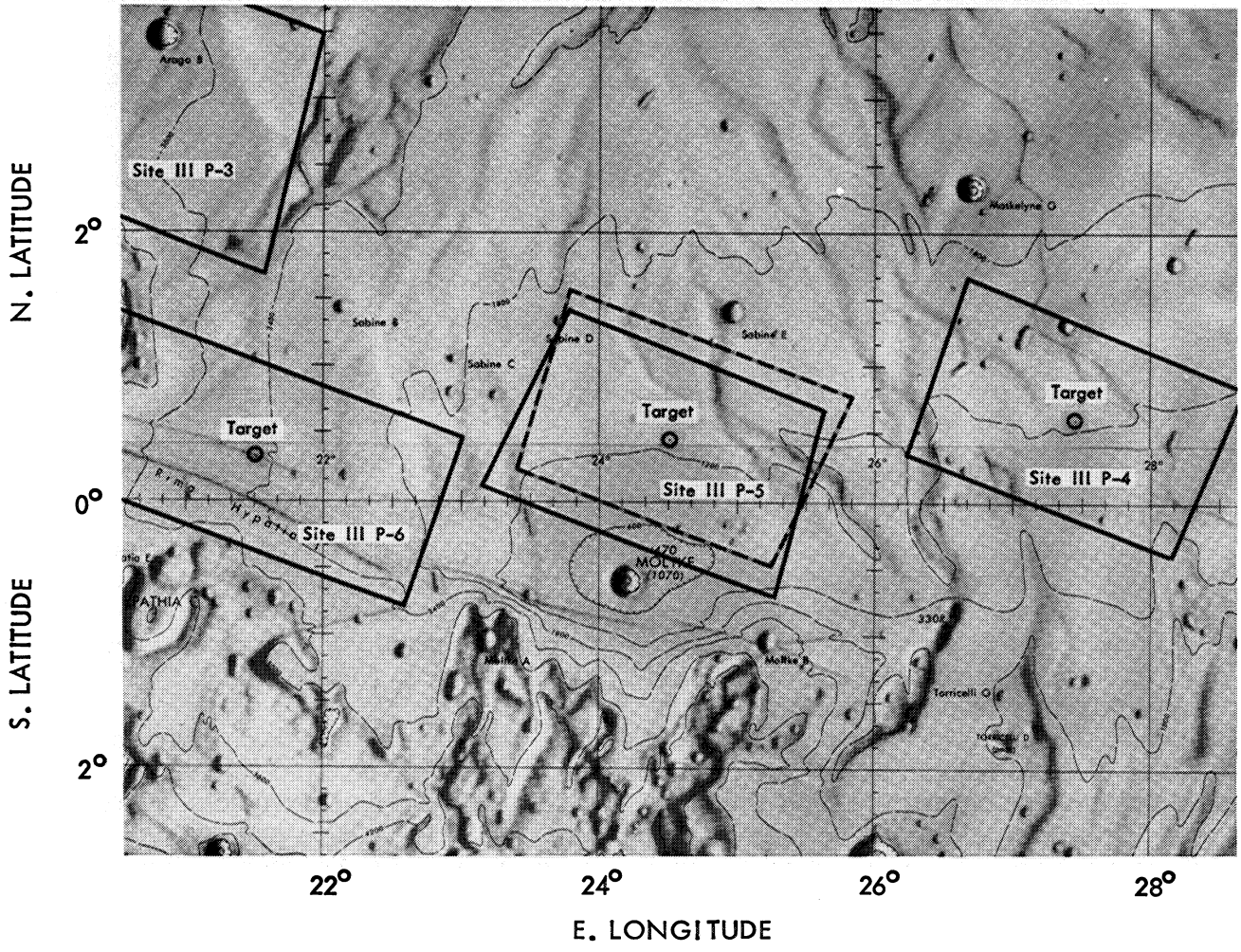

Figure 3-14: Coverage of Site IIIP-5; Inflight Prediction EVAL Computation

and sequenced in the fast mode with the camera axis near vertical on the second pass (Orbit 53). The area photographed is the vicinity of Ranger VIII impact in southern Mare Tranquillitatis. The area previously was photographed as part of Sites I-3 and IIP-6. Photographs were read out in priority mode only. Those frames obtained are diagrammed in Figure 3-15. Although photographed for convergent telephoto stereo so the photographs from each pass overlap, each sequence is shown separately for clarity in Figure 3-15.

The photographs from both sequences at this site appear to be considerably underexposed. The reconstructed framelets on positive GRE film have high average densities which tend to obscure lunar surface details near the resolution limit. On-axis detection of small craters spanning three to five scan lines is possible where image densities and signal-to-noise ratios are favorable. In off-axis framelets, where underexposure and lens transmission fall-off are both contributing factors, the resultant high-density images make detection of small surface features difficult.

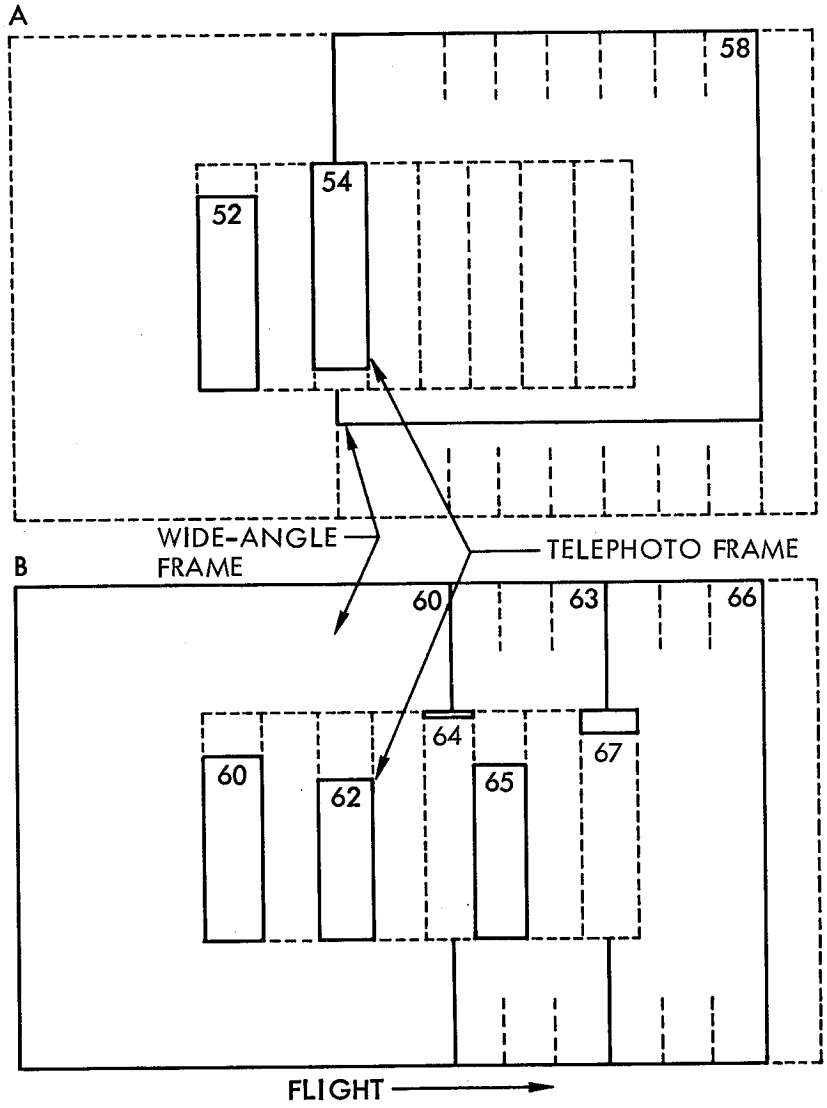

Note: Solid line outlines frames (or portions) readout.
Dashed lines outline frames photographed but not readout.

Figure 3-15: Priority Readout of Site IIIP-5

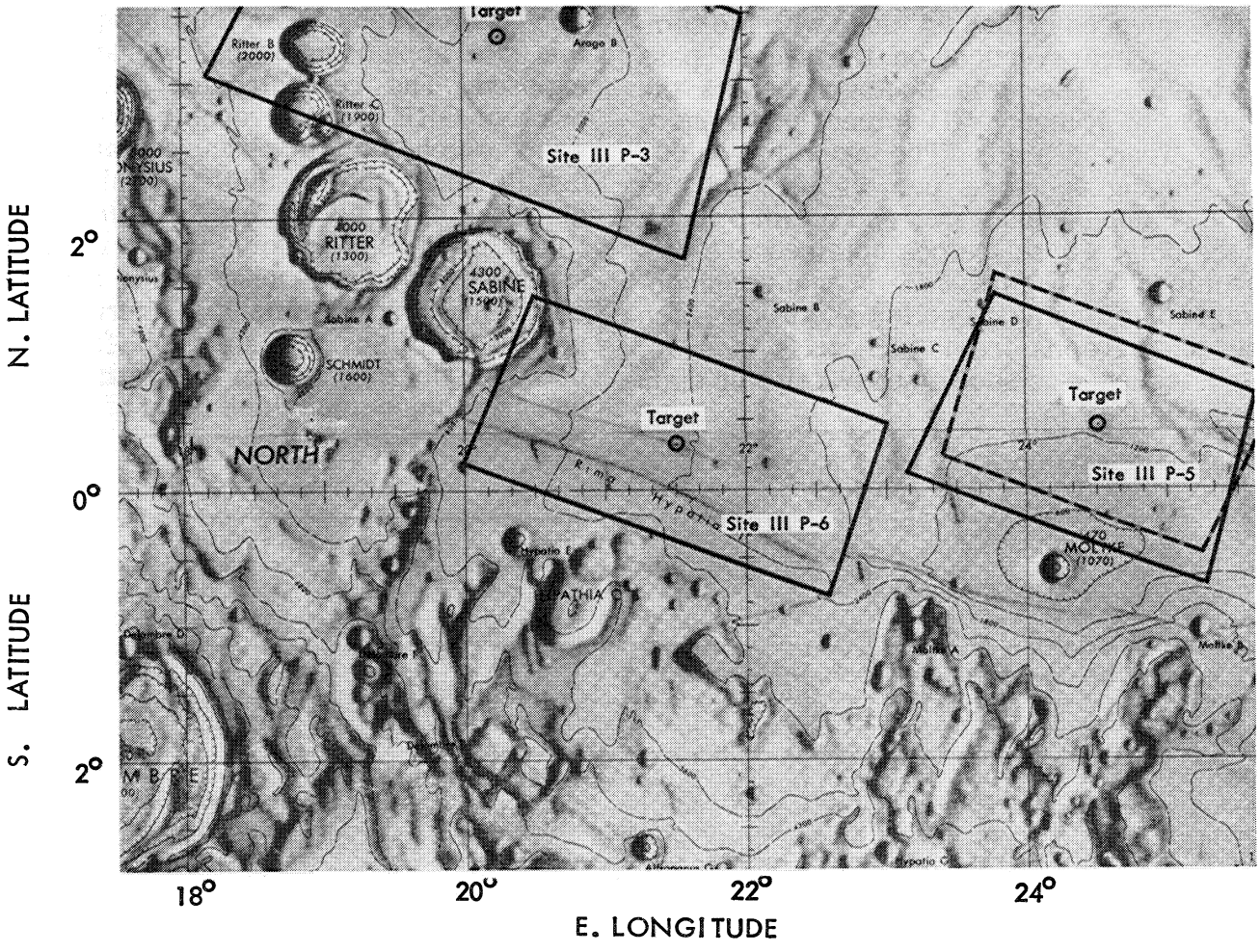

Figure 3-16: Coverage of Site IIIP-6; Inflight Prediction EVAL Computation

3.2.6 Site IIIP-6

The location of Site IIIP-6 was specified as 21°30′E, 0°20′N, with coverage as shown in Figure 3-16. The area is near the mare-upland contact southeast of Sabine, and includes the two broad parallel rilles, Rima Hypatia I and II. Although the area as shown on the charts (LAC 60 Julius Caesar, and AIC 60 C Arago) is represented as a mare area, the albedo is high (0.120) and Telephoto Frame 70 shows an area having a surface character more typical of low-relief upland. The wide-angle photographs of Frame 70, however, do not have the appearance of upland nor any comparable albedo differences.

Site IIIP-6 was photographed as a single sequence of four frames in the slow mode. The photographs of the site were read out in the priority mode only, as diagrammed in Figure 3-17.

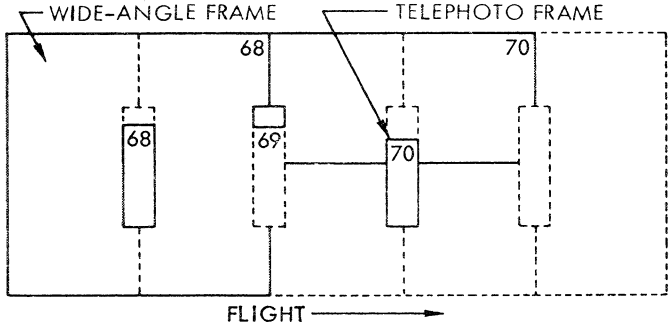

Note: Solid line outlines frames (or portions) readout.
Dashed lines outline frames photographed but not readout.

Figure 3-17: Priority Readout of Site IIIP-6

Telephoto and wide-angle photographs read out for Site IIIP-6 are considerably underexposed. Average image densities appear to be high. However, on-axis resolution was fairly satisfactory despite the dense images seen on positive film.

Craters spanning three to five scan lines can be discerned in the central areas of both telephoto and wide-angle frames. In retrospect, it appears that an exposure of 0.04 second would have resulted in better photographic quality than that obtained with the 0.02-second exposure actually used.

3.2.7 Site IIIP-7a and IIIP-7b

Site IIIP-7 also was planned for convergent telephoto stereo coverage. The point targets for sequences a and b were specified as 1°17′W, 1°02′N, and 1°20′W, 0°55′N, respectively. Sequence b was taken with the camera axis tilted to point at the site location from the nearest orbit, (Orbit 65) and sequence a was taken with cross-track tilt of 23.3 degrees for the convergent stereo. Sequence b was thus taken with the camera axis more nearly vertical (10 degrees).

The area photographed is near the central part of Sinus Medii, as shown in Figure 3-18, near Site IP-5, and between Sites IIP-7 and IIP-8. No major topographic features occur within the area although some low wrinkle ridges are present. The surface is quite rough on a small scale. The profusion of small craters produces a large number of small areas of hard shadow and adjacent bright highlights that give the photographs the appearance of overall high contrast. Some albedo variation within the site is apparent.

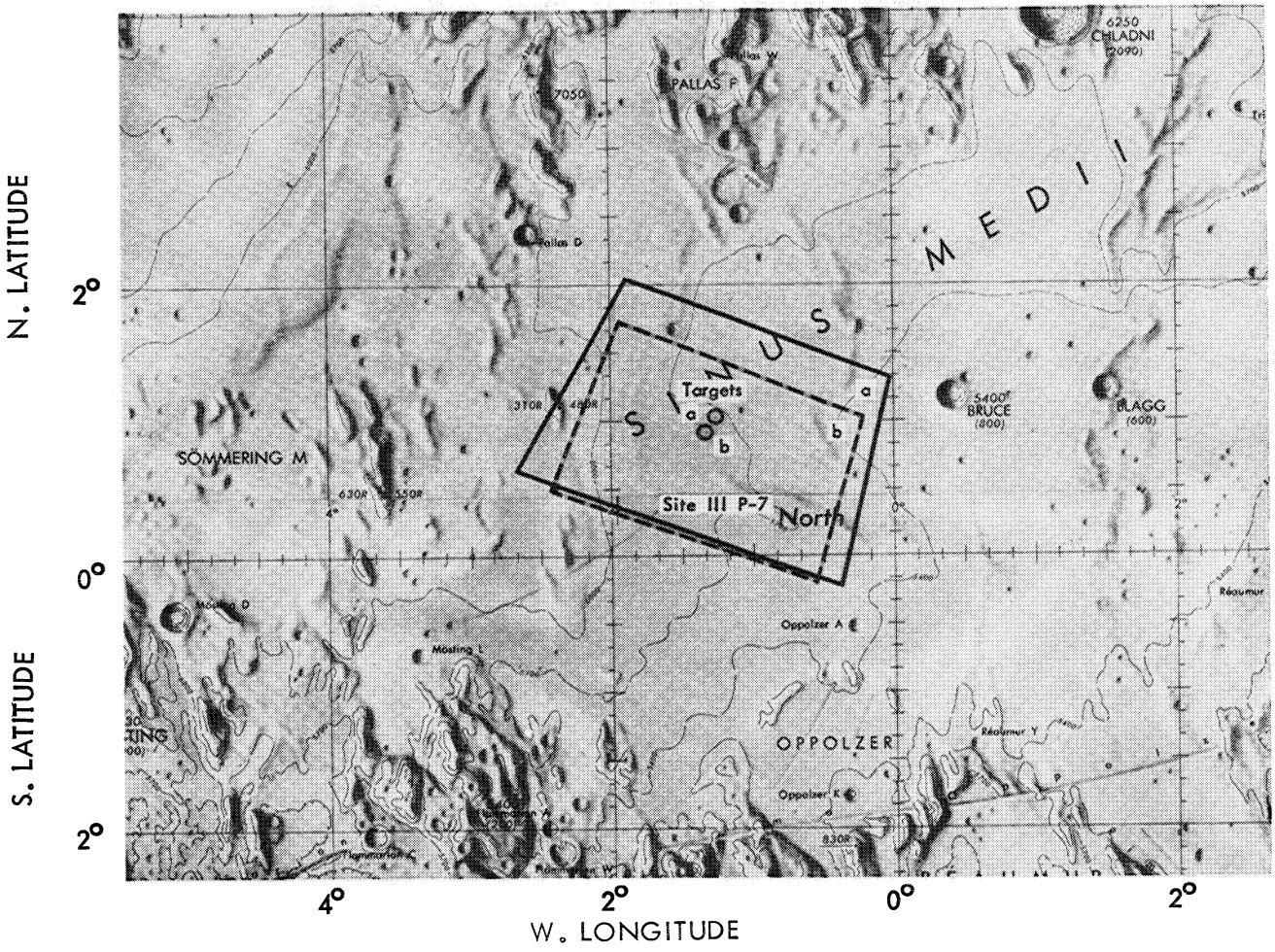

Figure 3-18: Coverage of Site IIIP-7; Postmission EVAL Computation

Site IIIP-7 and all subsequent primary sites were read out completely in final readout, thus the photographic coverage is complete.

The photographs obtained during both sequences were of very good photographic quality. The exposure of 0.04 second, used for both sequences, resulted in good contrast and definition in both wide-angle and telephoto frames (Figures 3-19 and -20). Although occasional frames were slightly underexposed because of variations in surface luminance, image densities were satisfactory. On-axis resolution was very good for both telephoto and wide-angle photographs in both sequences. Craters which spanned only three scan lines could be detected in the central areas of these frames.

Resolution such as this appears to meet or exceed specified on-axis resolution limits, although the signal-to-noise ratio was not determined. The 80-mm wide-angle lens appears to be capable of slightly better on-axis image quality than the 610-mm telephoto lens. Near resolution limits, images formed by the 80-mm lens have slightly better contrast and definition than those formed by the 610-mm lens.

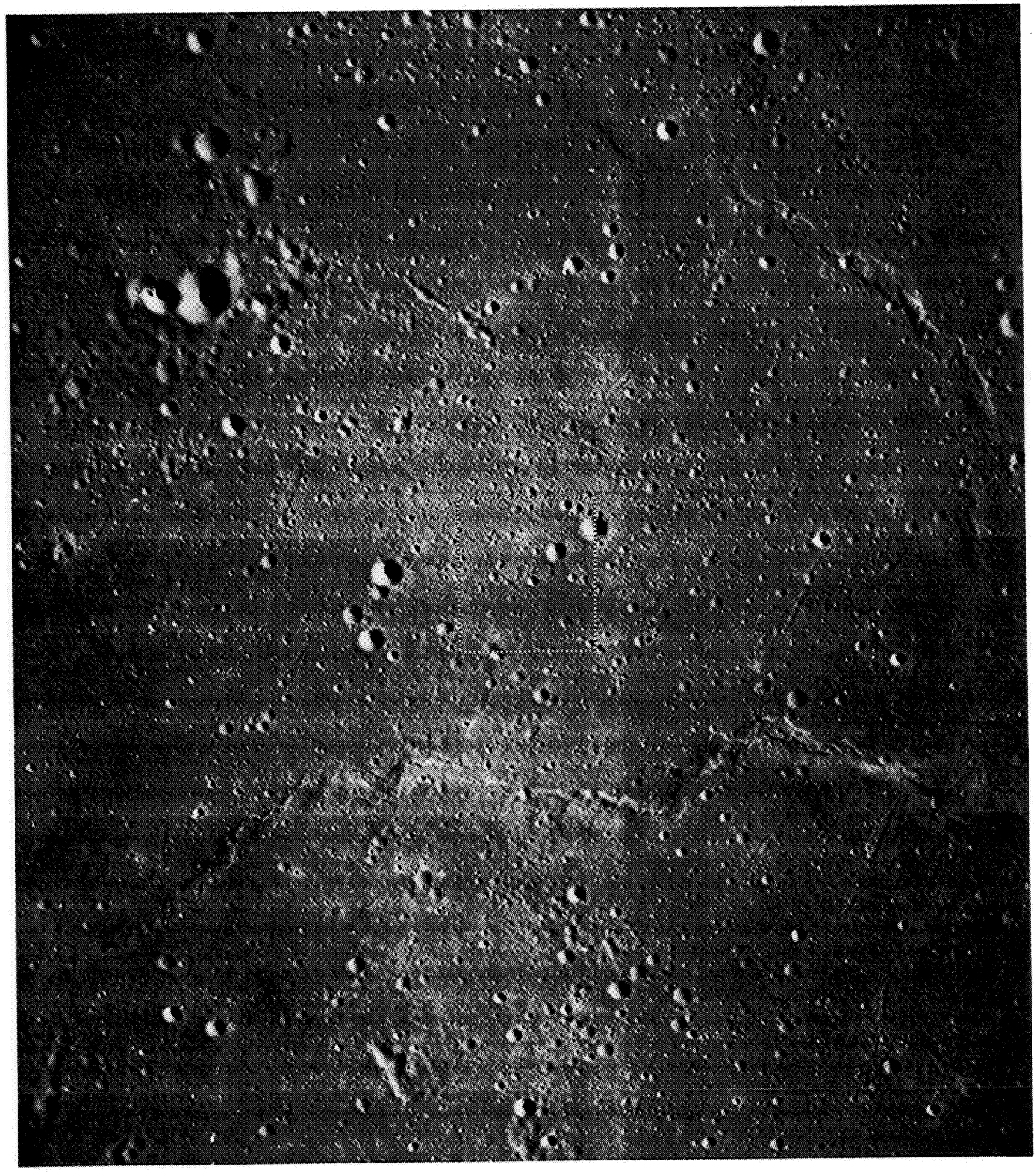

Figure 3-19: Site IIIP-7b Wide-Angle Frame 100

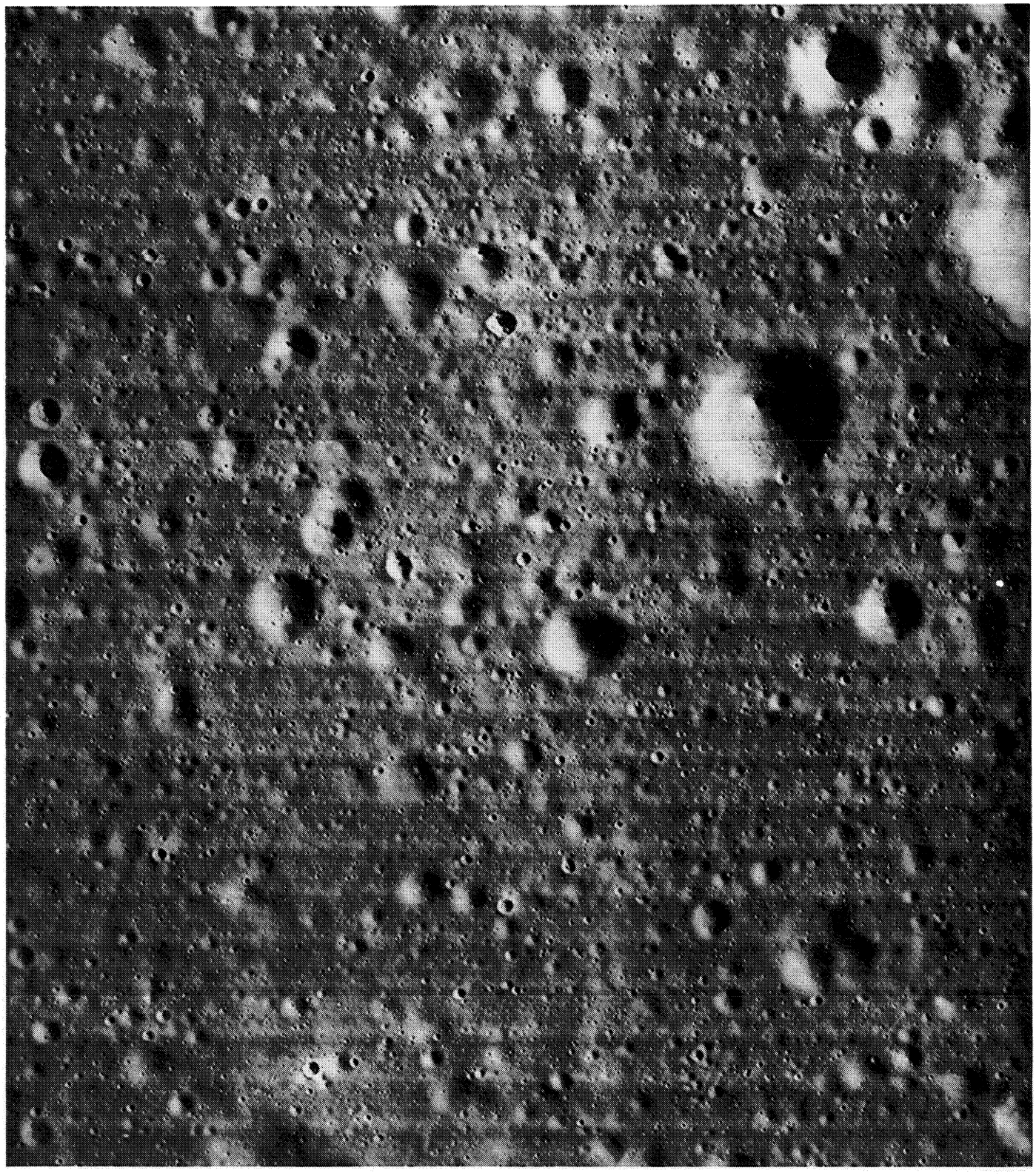

Figure 3-20: Site IIIP-7b Central Portion of Telephoto Frame 100

3.2.8 Site IIIP-8

This site, specified as 19°50′W, 0°50′S, spans a mare-type area south of Gambart A and includes much of the area photographed as Site IIP-11. Upland-type terrain occurs at both the western and eastern limits of the area photographed, as shown on Figure 3-21. The site is within the area of Copernican ray structure and includes some hummocks. The mare is generally flat but moderately rough at a small scale as seen on the wide-angle photographs (e.g., Frame 126, Figure 3-22). The upland area is more rugged and the slopes result in a wider range of surface luminance, part of which may be due to albedo variation associated with the ray structure. This may be seen in Frame 130, Figure 3-23. The wide luminance range associated with the upland terrain is also evident in the telephoto photographs, but detail is lost only at either extreme, as illustrated in a portion of Telephoto Frame 130, Figure 3-24.

Telephoto and wide-angle frames for this site were of good photographic quality. The exposure of 0.04 second used for the fast eight-frame sequence resulted in photographs with good contrast and definition. Near-optimum densities were obtained in the central frame areas. On-axis resolution in wide-angle frames permitted the detection of craters spanned by three scan lines. In telephoto frames also, craters included in only three scan lines could be discerned. Off-axis resolution, as in the end framelets where average densities tend to be higher, was usually about four to six scan lines.

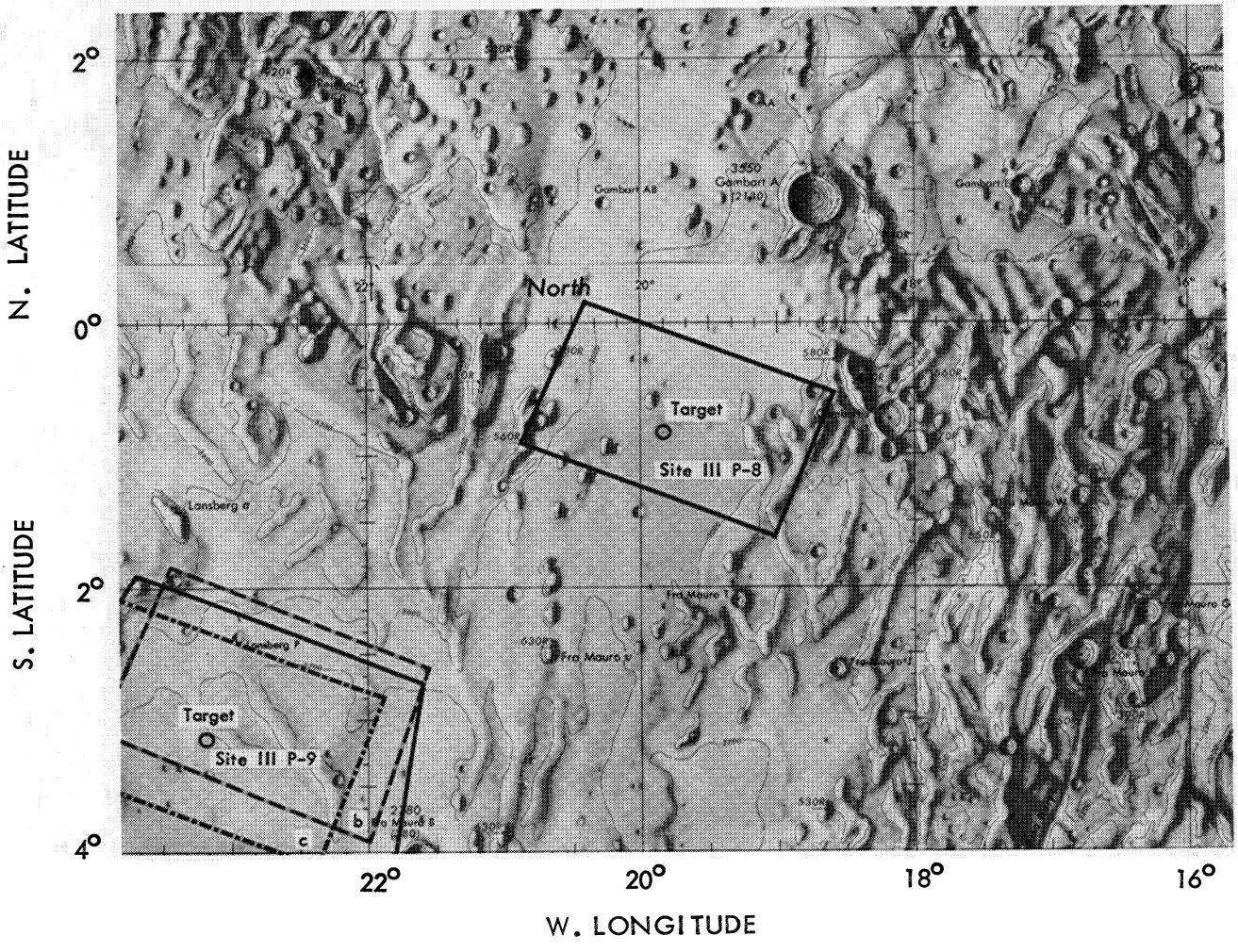

Figure 3-21: Coverage of Site IIIP-8; Postmission EVAL Computation

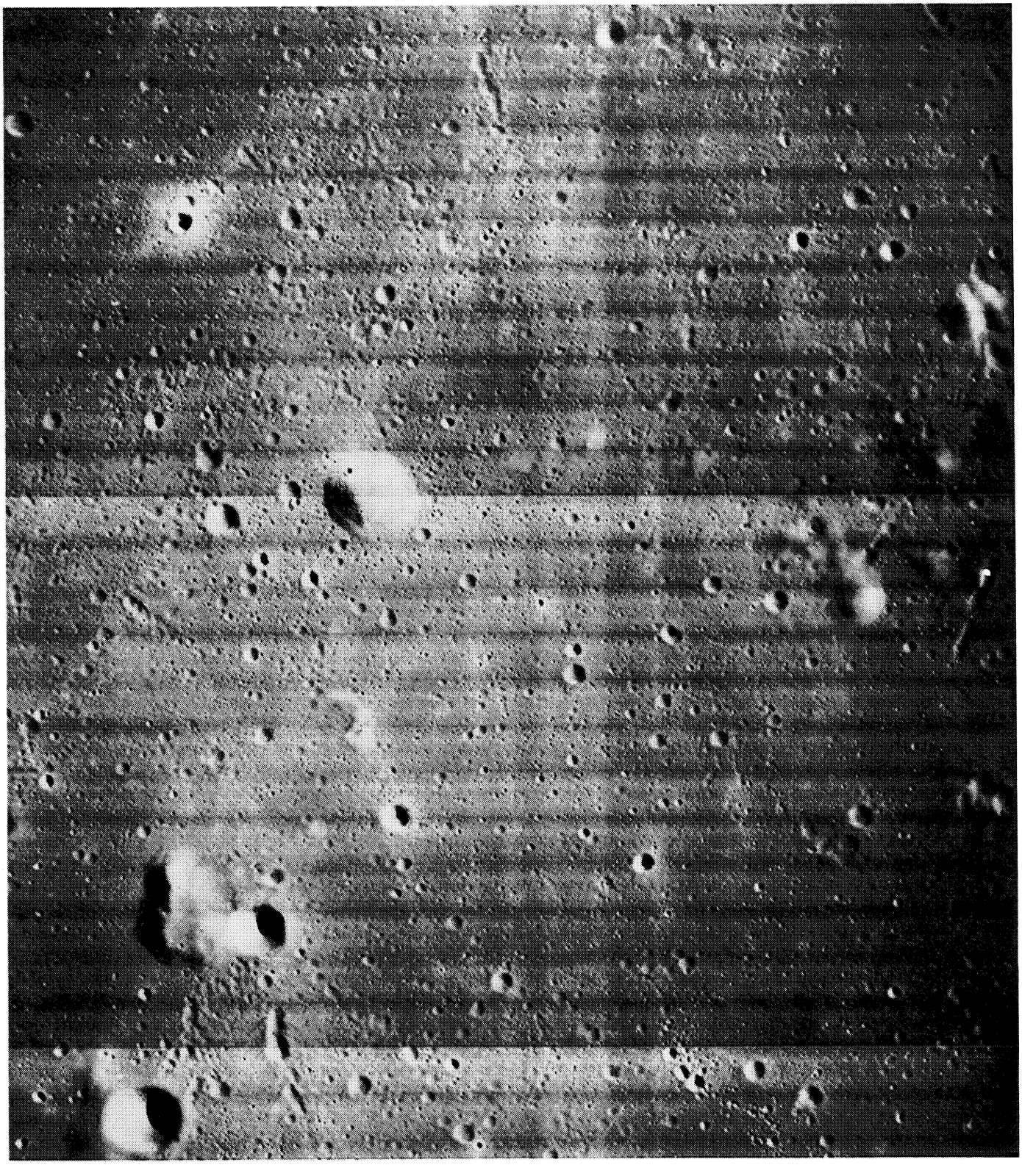

Figure 3-22: Site IIIP-8 Wide-Angle Frame 126

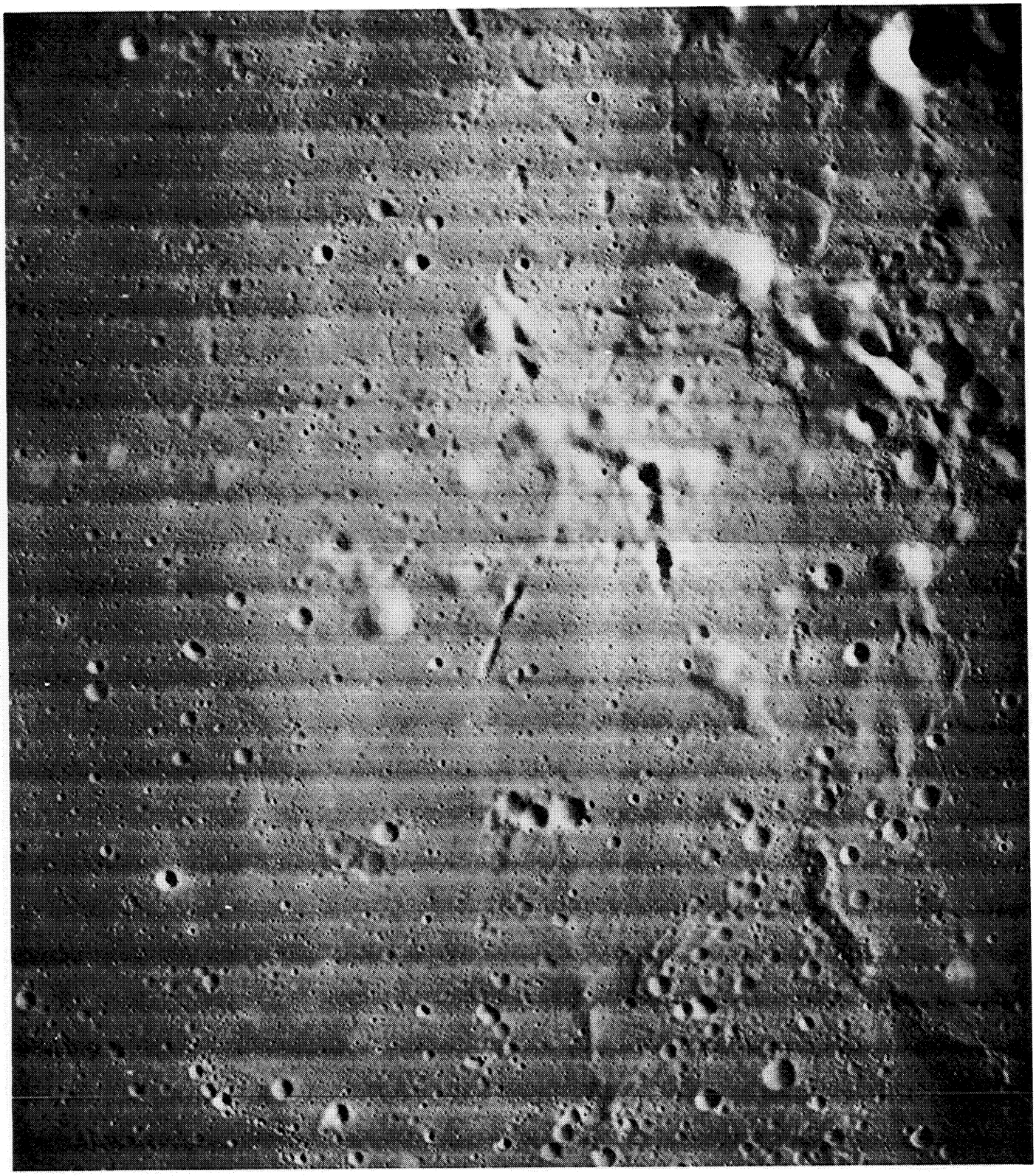

Figure 3-23: Site IIIP-8 Wide-Angle Frame 130

Figure 3-24: Site IIIP-8 Southern Portion of Telephoto Frame 130

3.2.9 Sites IIIP-9a, IIIP-9b, and IIIP-9c

Site IIIP-9 is located in a mare area southeast of Lansberg. The position specified was 23°11′W, 3°09′S, within the area of Site IP-7. The area is mostly flat mare with some low ridges. Some hills are included in the western limits of the site coverage.

The site was photographed by three sequences of eight exposures taken in the fast mode. The photographic procedure to be used for the site was specified by U.S. Government Memorandum 10M-67-292-ATY/NLC as follows.

- P-9a - "Southern edge of coverage shall aline approximately with the southern edge of the P-9c coverage."
- P-9b - "Overlap 10 - 15% with the P-9c coverage."
- P-9c - "Camera pointed at site from nearest orbit."

This procedure was specified to ensure coverage of the area planned for Surveyor III landing, and to obtain high-resolution convergent stereo. The coverage obtained is shown plotted in Figure 3-25.

The wide-angle photography was quite uniform over the principal part of the site. The change in exposure from 0.02 second for the first sequence to 0.04 second for the second and third resulted in satisfactory exposure. Examples of these photographs are illustrated in Figures 3-26, -27, and -28 taken from the successive orbits.

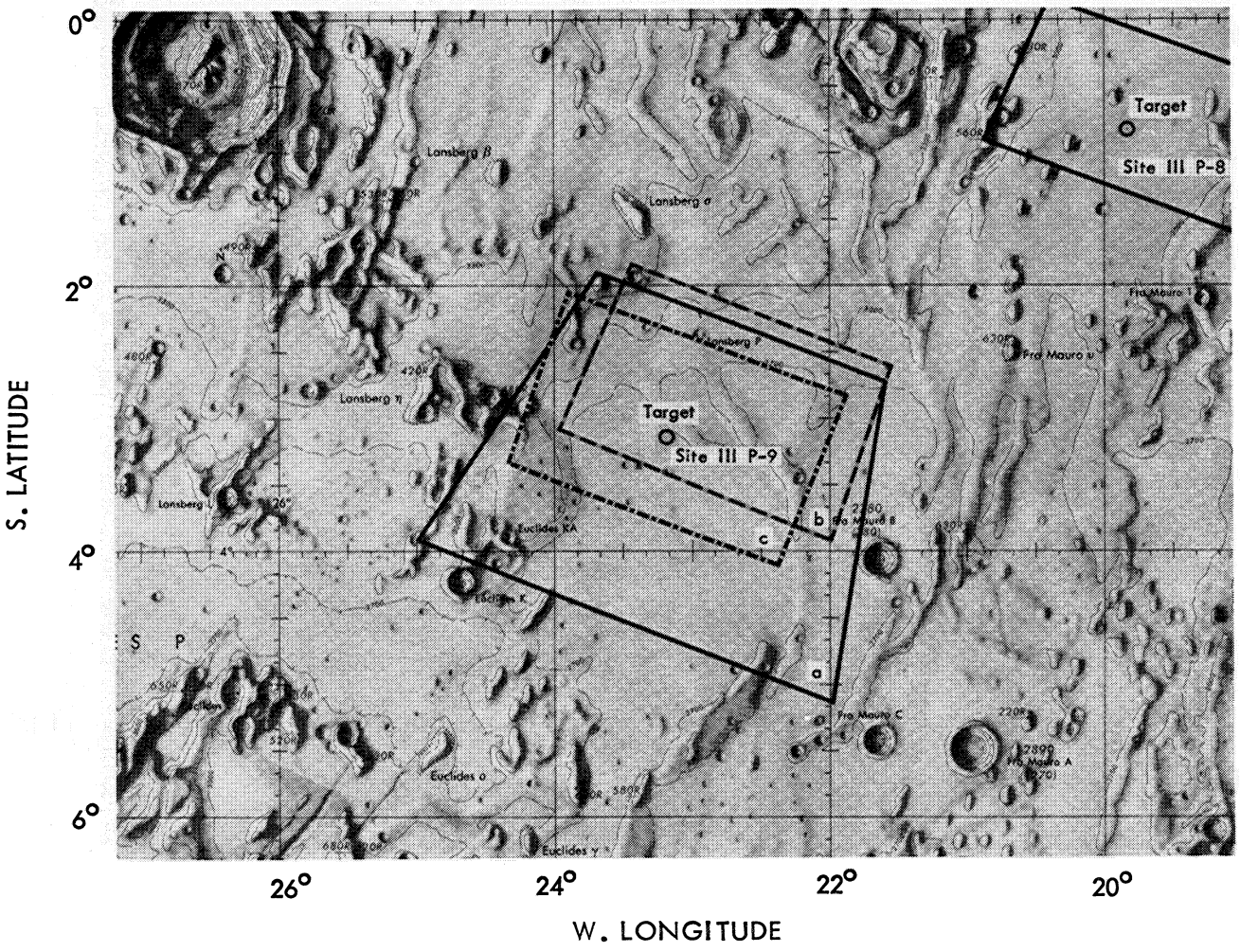

Figure 3-25: Coverage of Site IIIP-9; Postmission EVAL Computation

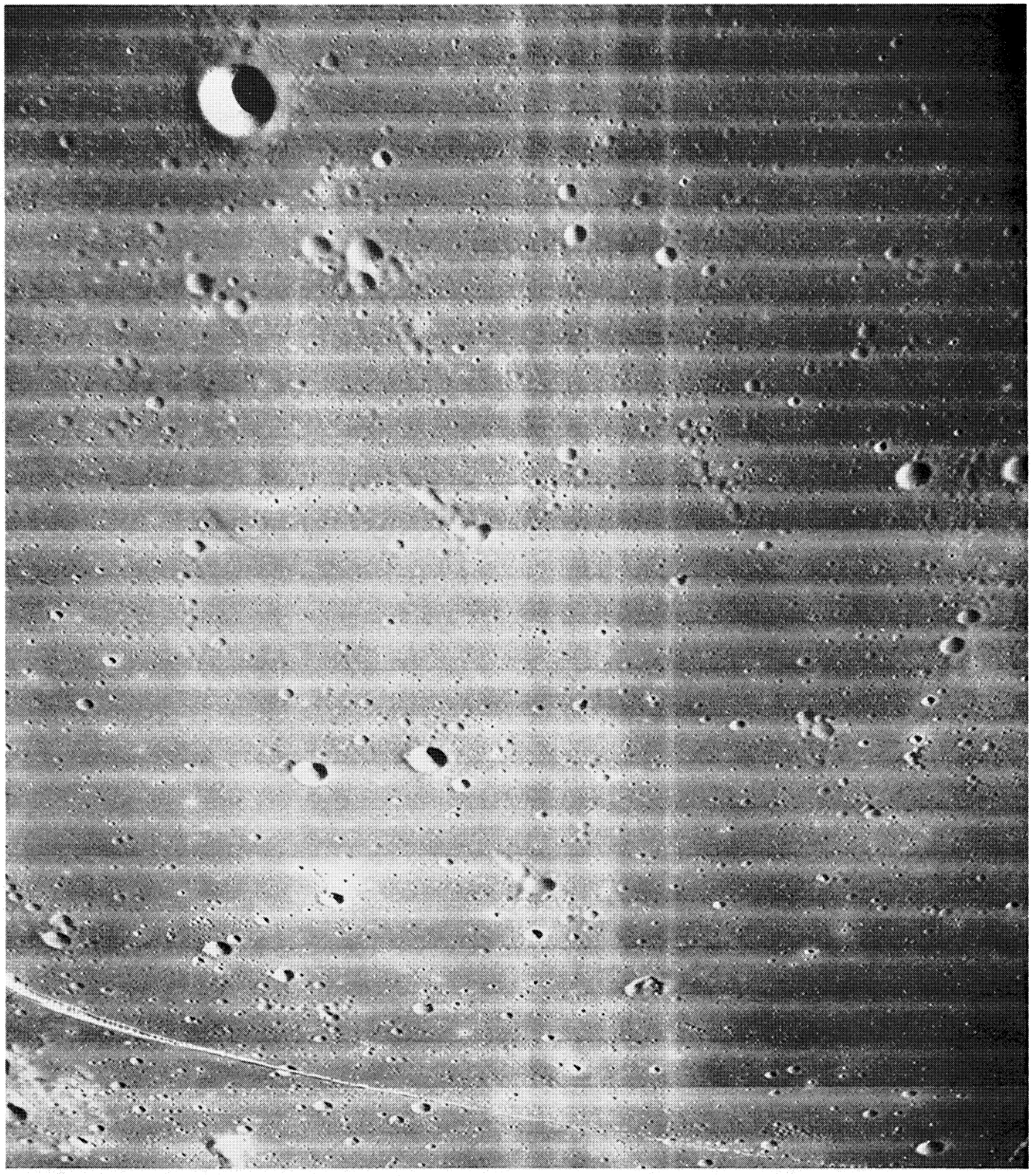

Figure 3-26: Site IIIP-9a Wide-Angle Frame 140

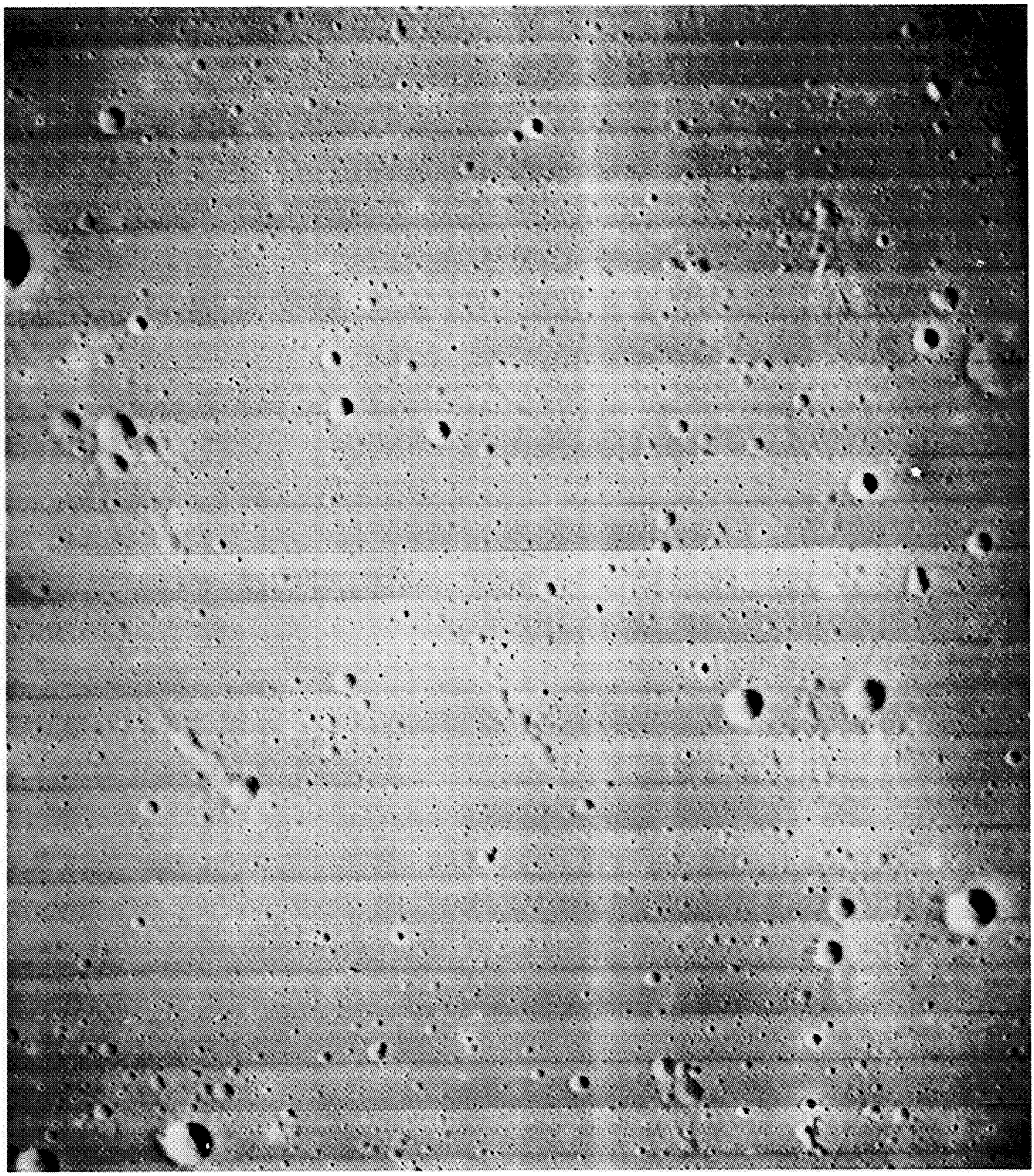

Figure 3-27: Site IIIP-9b Wide-Angle Frame 149

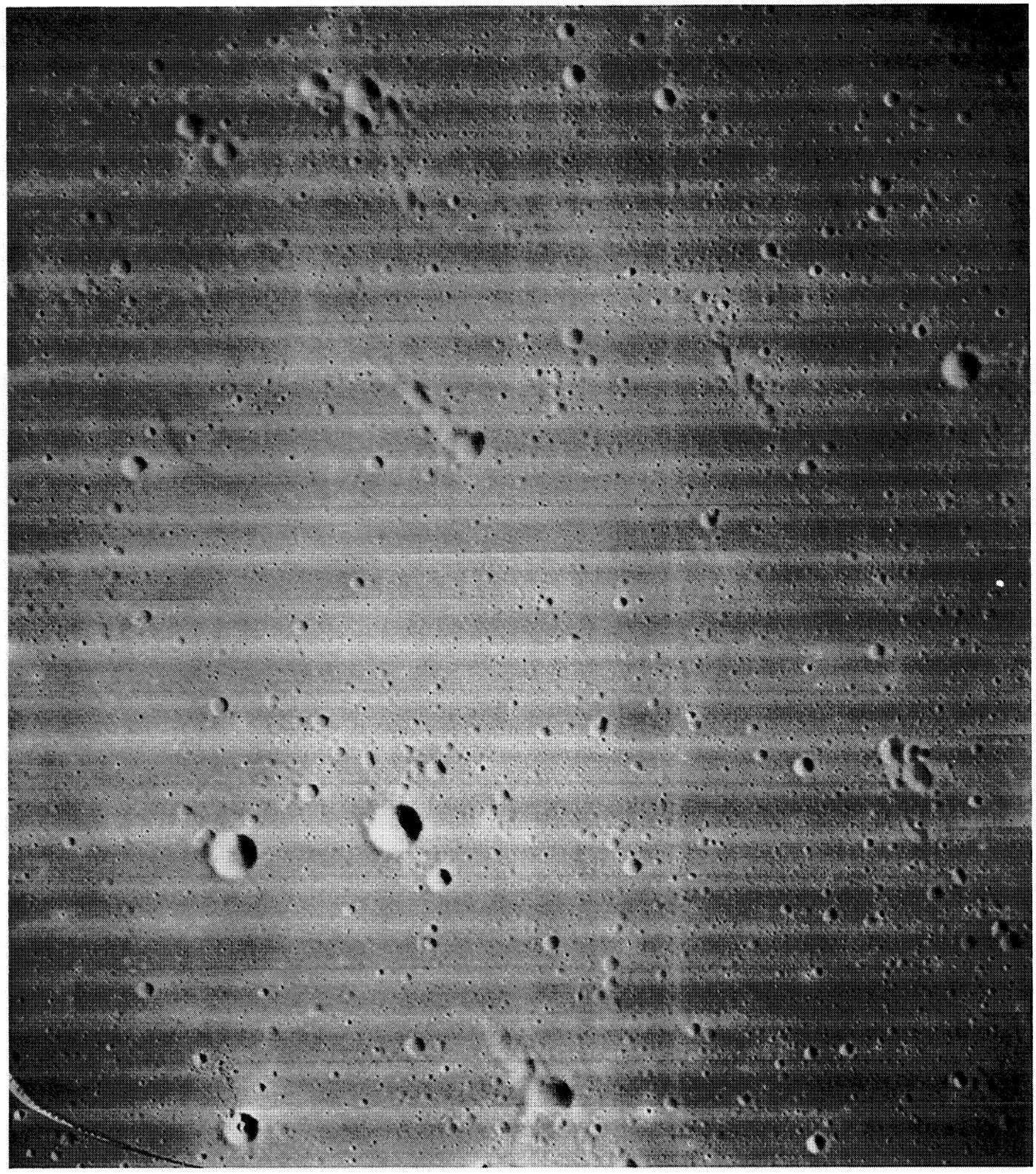

Figure 3-28: Site IIIP-9c Wide-Angle Frame 157

The photographs of Site IIIP-9a were fairly satisfactory except for underexposure. The exposure of 0.02 second resulted in relatively high average densities in both wide-angle and telephoto frames. The underexposure, coupled with lens off-axis transmission fall-off, caused very dense images and loss of detail in end framelets and frame corners.

In some instances, off-axis densities were most satisfactory where brighter lunar features were included in the frame ends or corners. On-axis resolution was good for both wide-angle and telephoto frames. Lunar surface details spanning approximately three to four scan lines could be identified in the central areas of these photographs.

As a result of the increased exposure time of 0.04 second used for IIIP-9b and IIIP-9c instead of the 0.02 second used on the first pass, the photographs had near-optimum film image characteristics. The photographic quality of the frames in these two sequences was very good. Resolution was excellent in both telephoto and wide-angle frames. Craters and projections with cross sections corresponding to three scan lines could be identified in the center portions of the photographs. Off-axis resolution was also satisfactory. Lunar features spanning only four to five scan lines could be detected in the end framelets. An example of the telephoto photograph from Site IIIP-9c is shown in Figure 3-29.

At the time this report was being prepared, Lunar Orbiter and Surveyor III photographs were being correlated to obtain more precise location of the latter and to correlate terrain characteristics. Figure 3-28a is Wide-Angle Frame 136 showing the location of the landing site. Figure 3-28b, Wide-Angle Frame 154, shows the landing area inscribed by a square. Figure 3-28c is an enlarged portion of Telephoto Frame 154 indicating the position of the Surveyor III spacecraft as determined by comparing rocks and craters visible in the Lunar Orbiter photograph with those shown in the Surveyor III photographs as indicated in Figure 3-28d. As a matter of interest, Figure 3-28d is an enlargement equivalent to about 100 diameters from the spacecraft film.

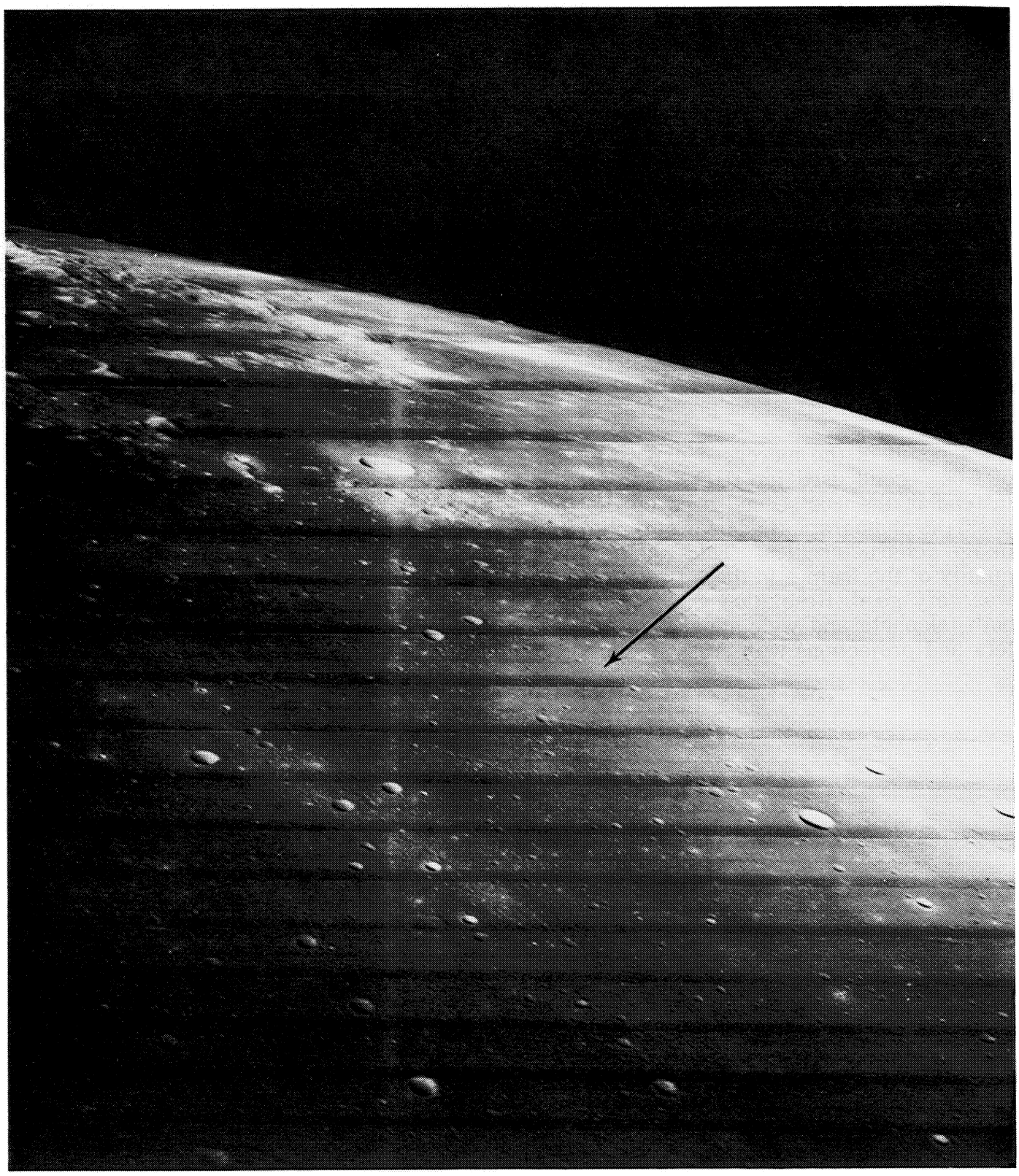

Figure 3-28a: Area of Surveyor III Landing

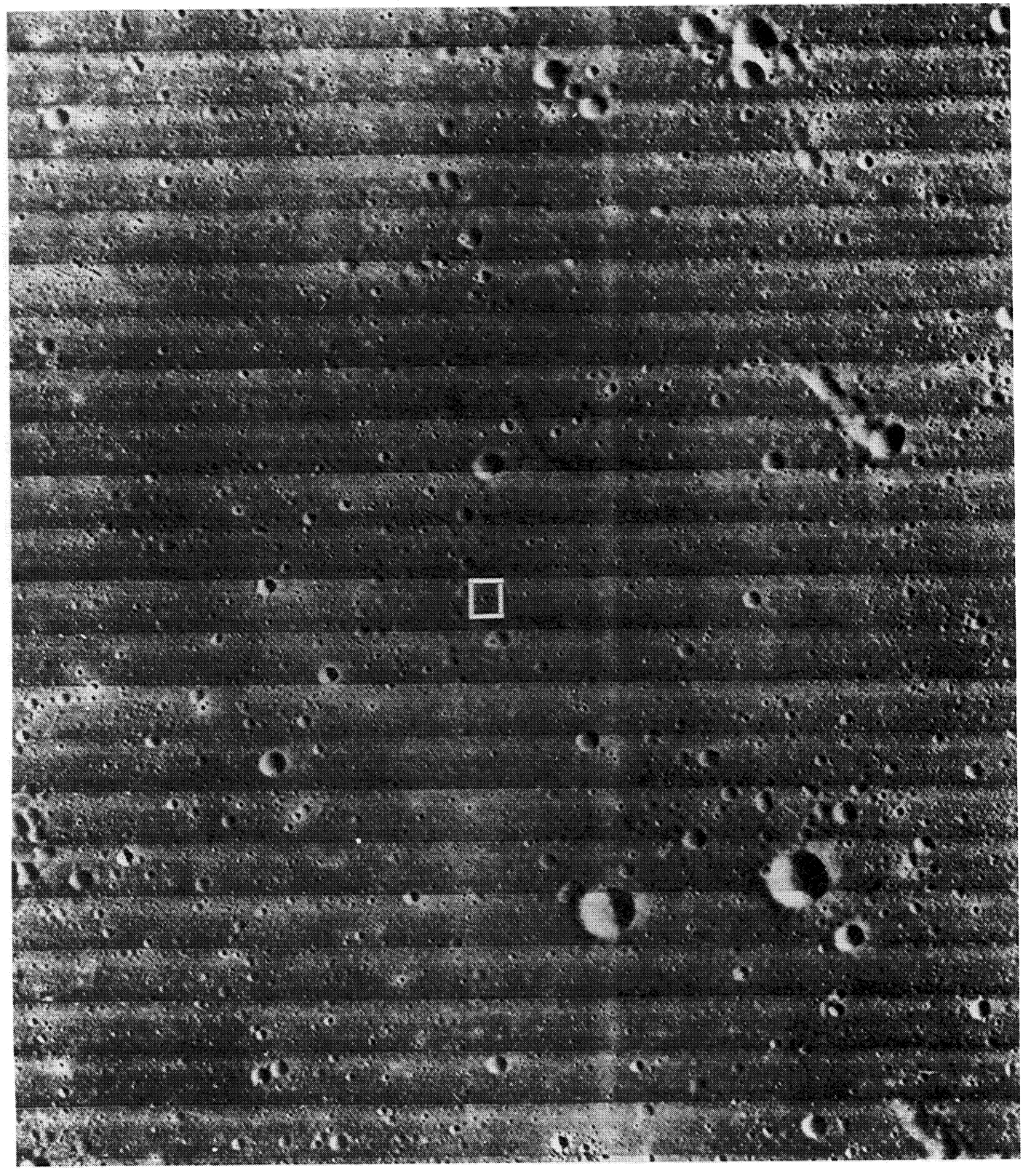

Figure 3-28b: Position of Surveyor III Landing Shown in Lunar Orbiter Frame M154

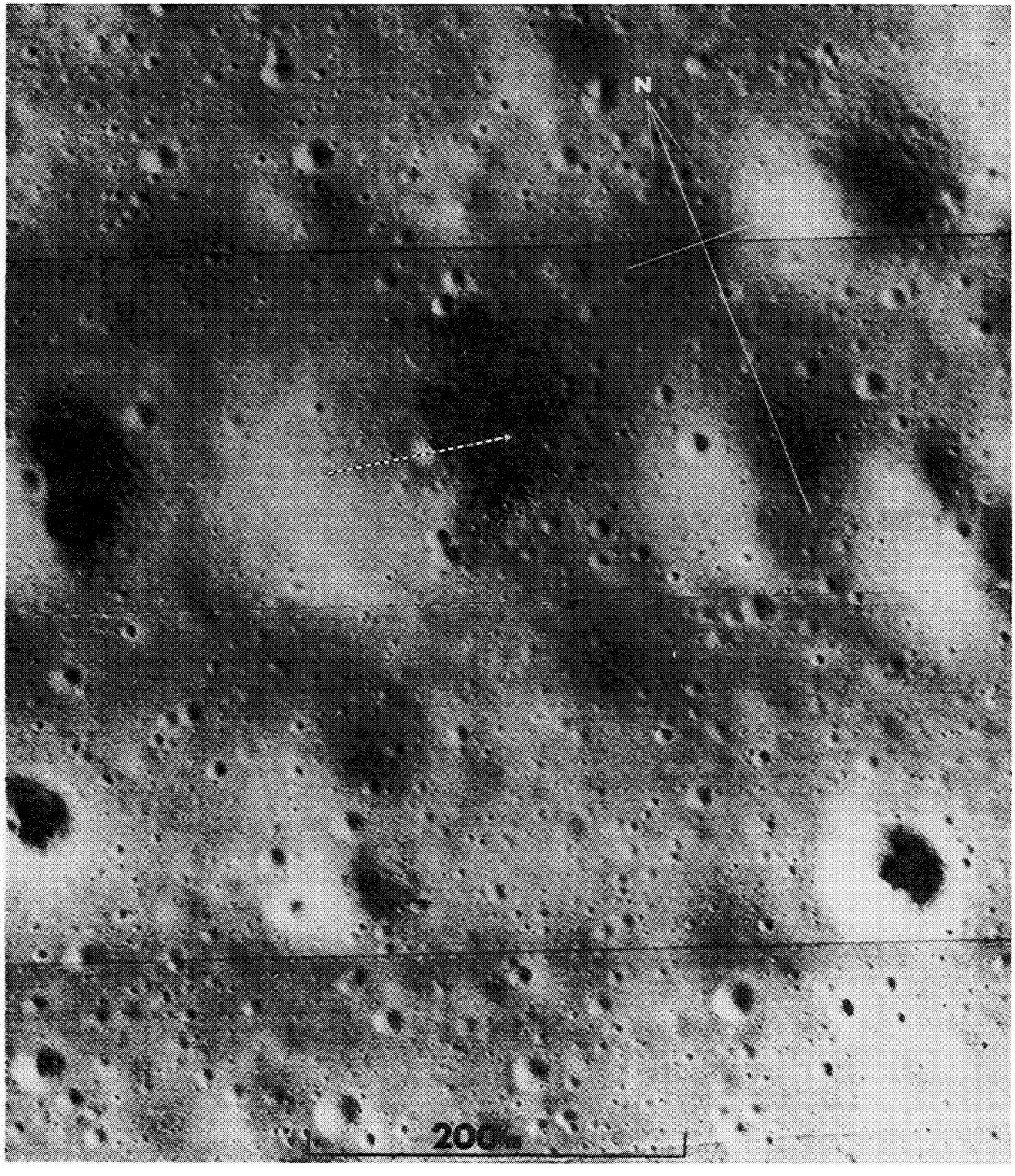

Figure 3-28c: Location of Surveyor III in Crater

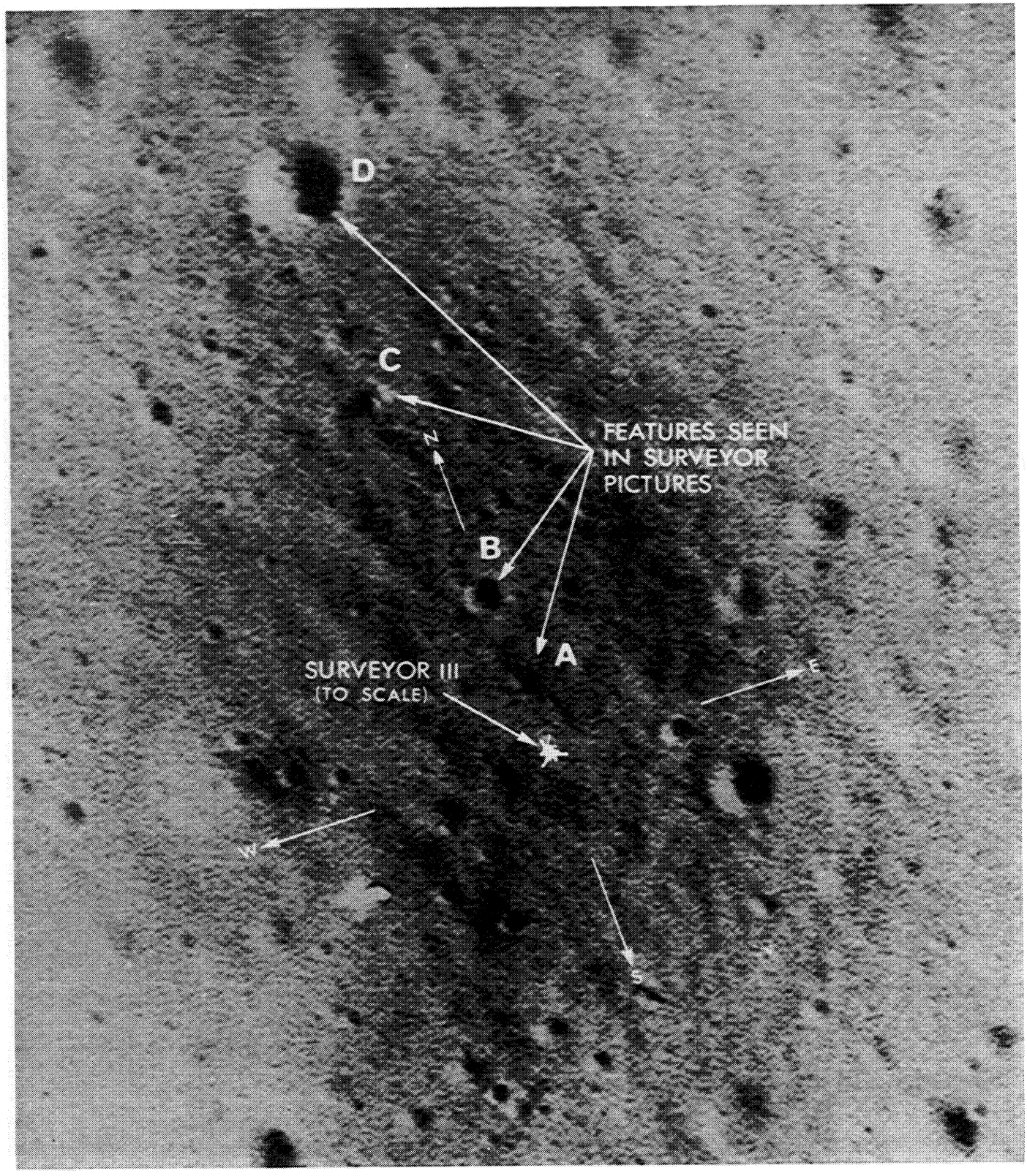

Figure 3-28d: Features used to establish Surveyor III Position

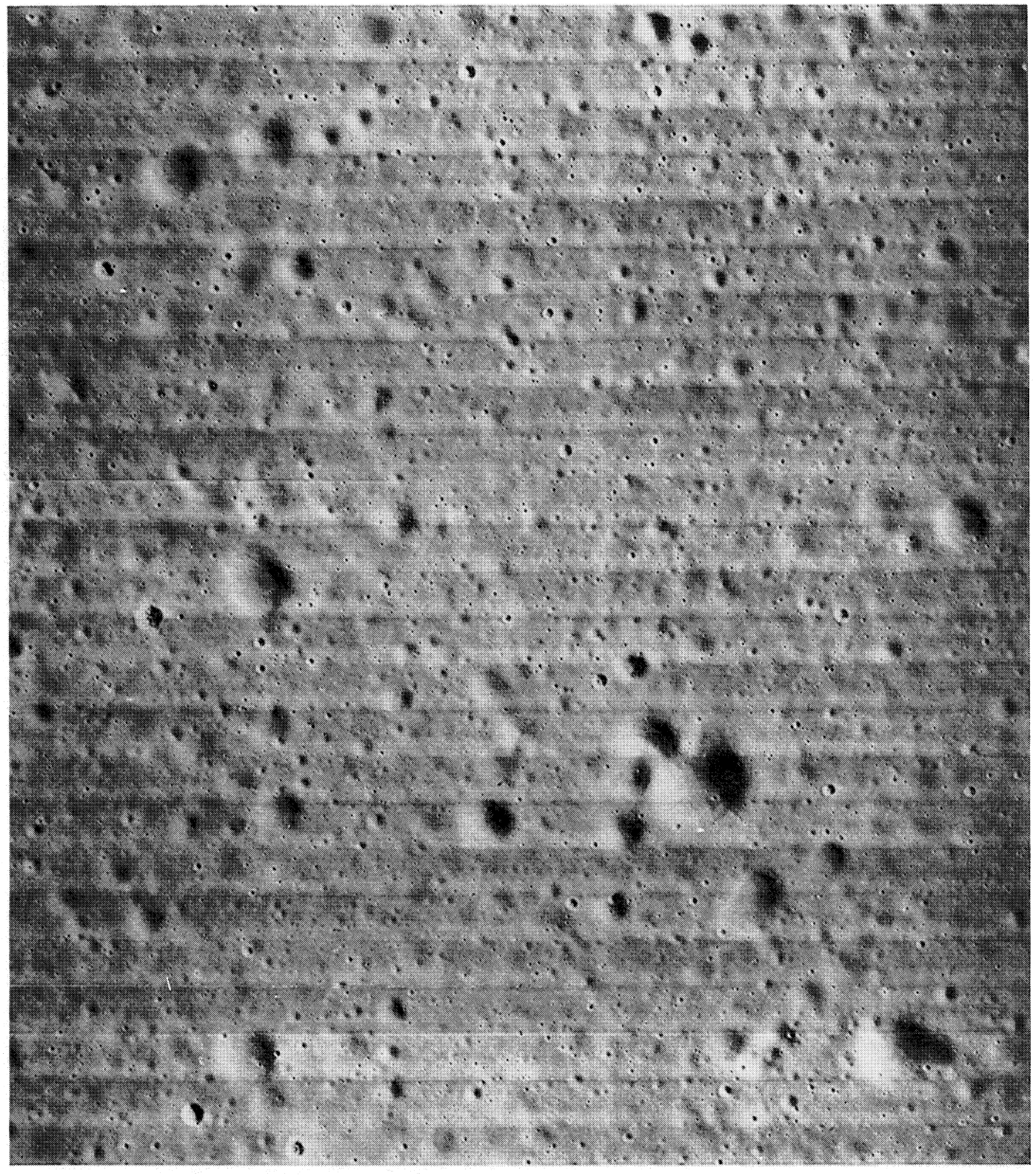

Figure 3-29: Site IIIP-9c Central Portion of Telephoto Frame 157

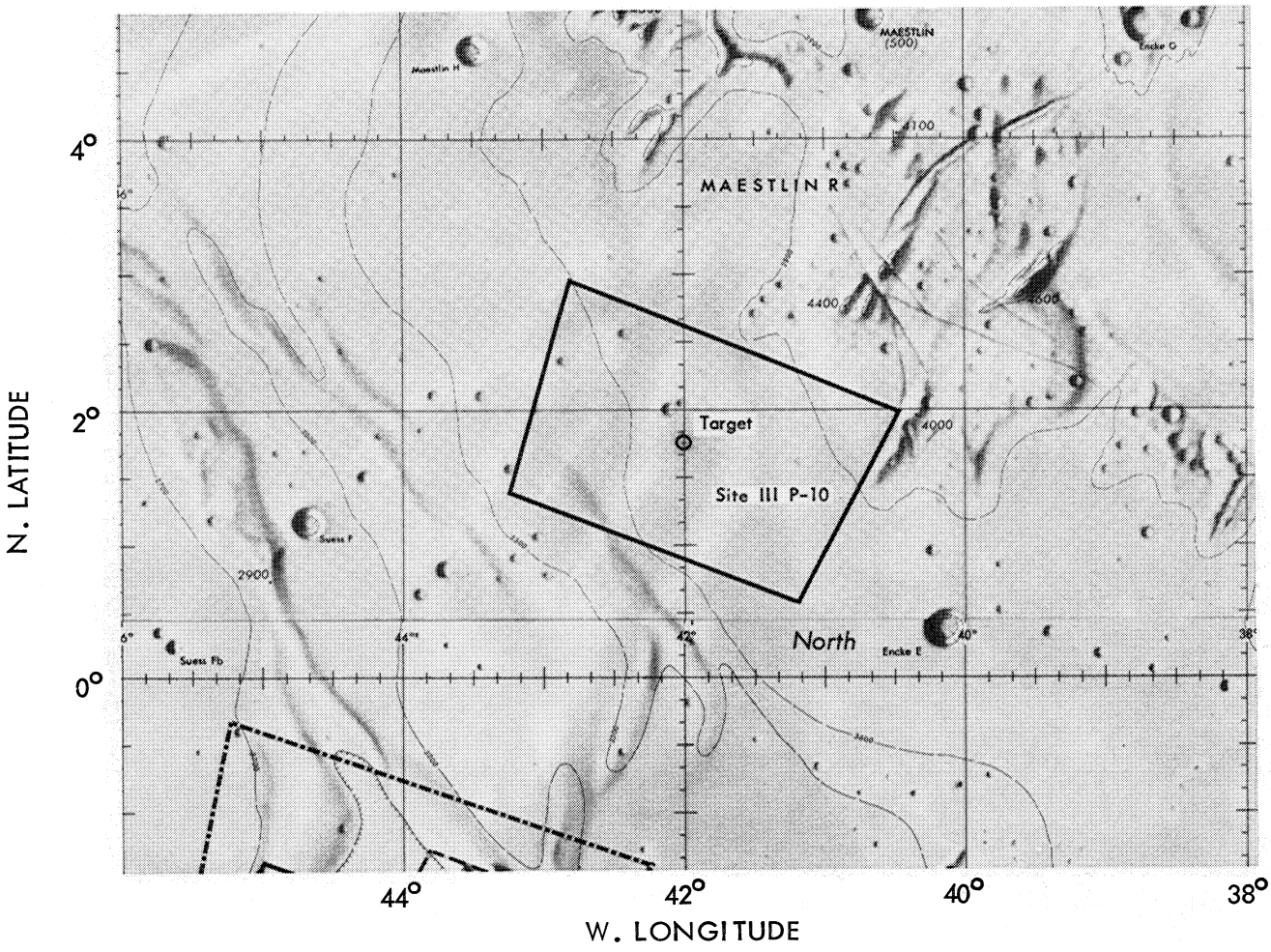

Figure 3-30: Coverage of Site IIIP-10; Postmission EVAL Computation

3.2.10 Site IIIP-10

This site, located at 42°00′W, 1°45′N, was planned to provide telephoto convergent stereo in conjunction with the photographs of Site IIP-13. One sequence of eight frames was exposed in the fast mode. The coverage obtained is plotted in Figure 3-30. Site IIP-13 also has been included for comparison. The apparent skew of coverage by the two missions is produced by the difference in orbit inclinations—approximately 12 degrees during Mission II and 21 degrees during Mission III.

The area is a very flat mare, but marked by numerous groups of secondary craters. Site IIIP-10 is within the ray system of Kepler, which accounts for the presence of ray structures and an apparent variation of albedo. The numerous small craters and relatively higher albedo of the areas of secondary impacts produce the appearance of overall high contrast, as seen in Figure 3-31. The telephoto coverage is of good quality, as represented by Figure 3-32.

Although the maximum exposure time of 0.04 second was used, the combination of lunar surface characteristics, phase angle, and illumination geometry existing at the time of photography resulted in low luminance and considerable underexposure. When viewed on positive film, frame centers were fairly dense and frame ends were often very dark, with consequent loss of detail. On-axis resolution was fairly satisfactory for both wide-angle and telephoto exposures. Surface features included in three to four lines could be detected in central areas of these photographs.